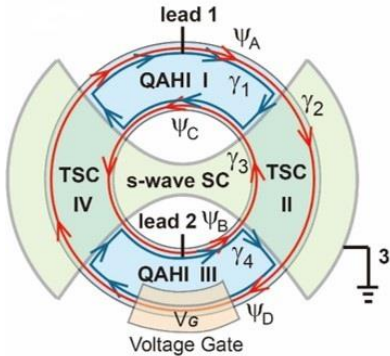


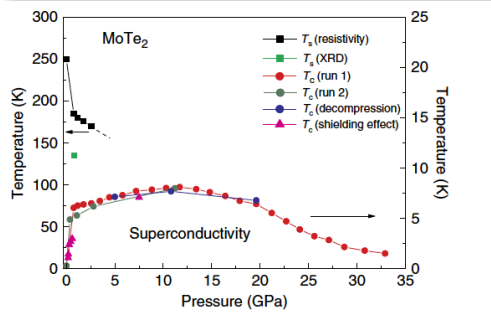
Magnetic Weyl Semimetals



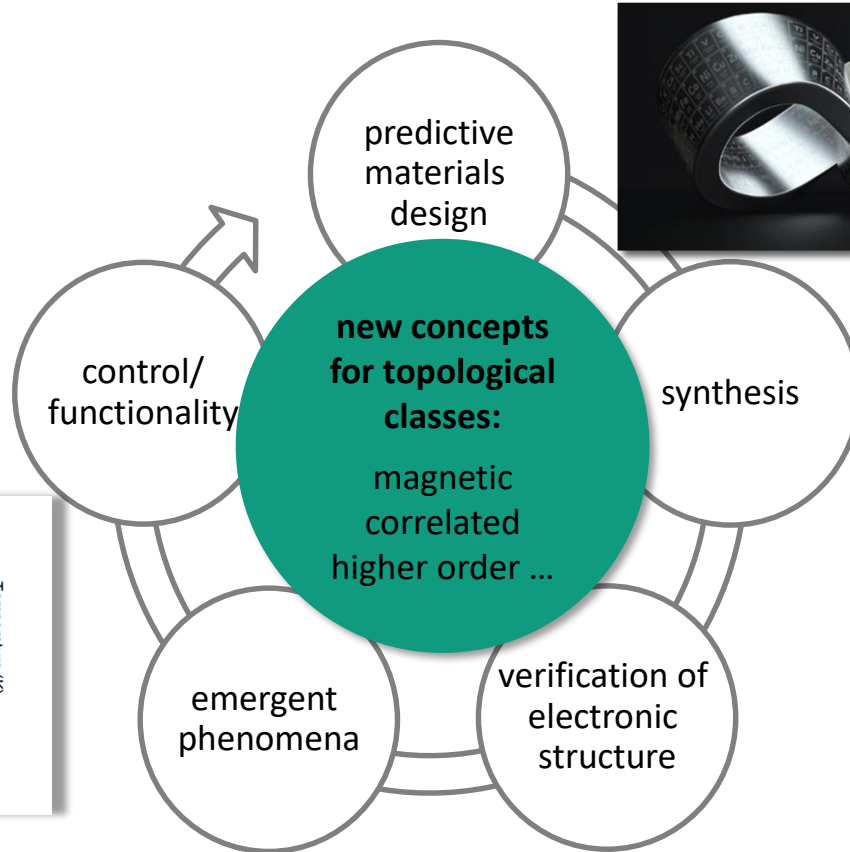
the concept



Lian, et al., PNAS 2018

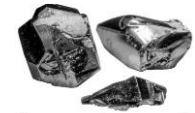


Qi et al. Nat. Com. (2016)

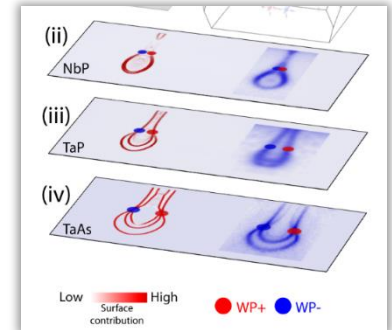


Topological quantum chemistry
Bradlyn, et al., Nature 2017
1807.10271, 1807.08756

© Nature



0 5 10
length (mm)

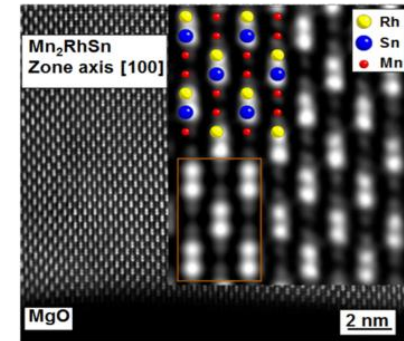
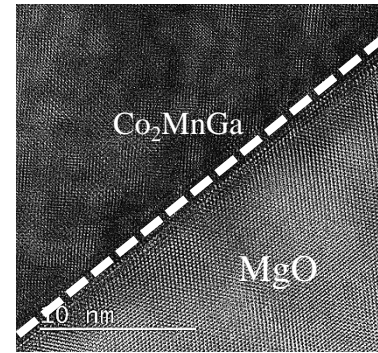
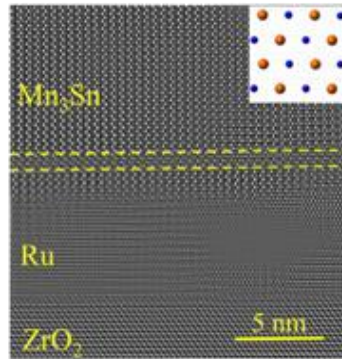
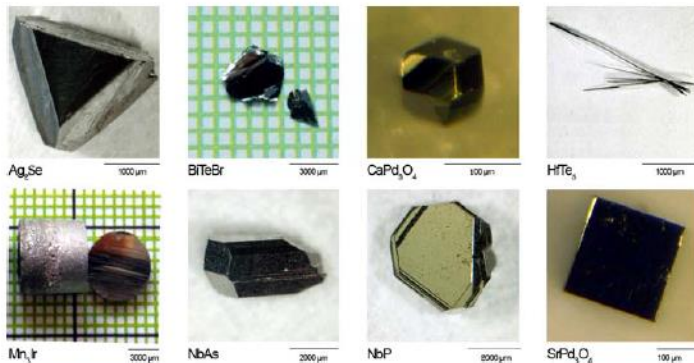
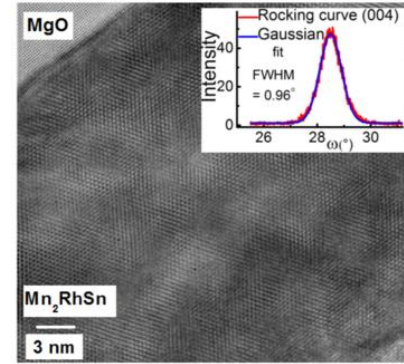


Liu et al. Nat. Mat. (2016)

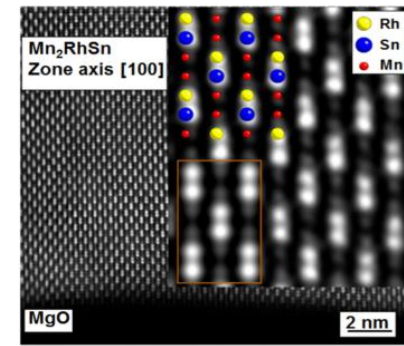
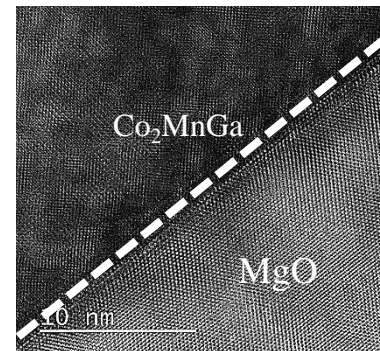
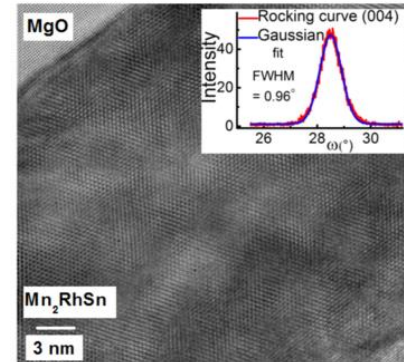
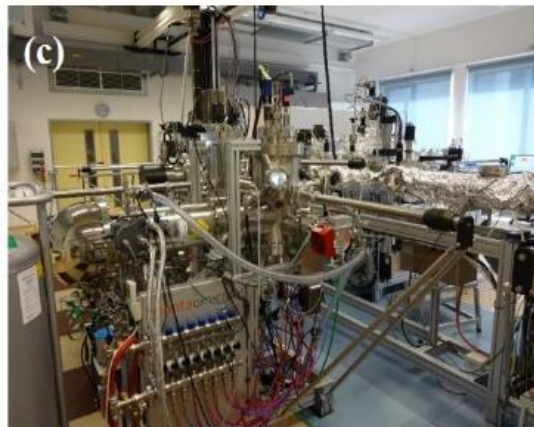
the materials

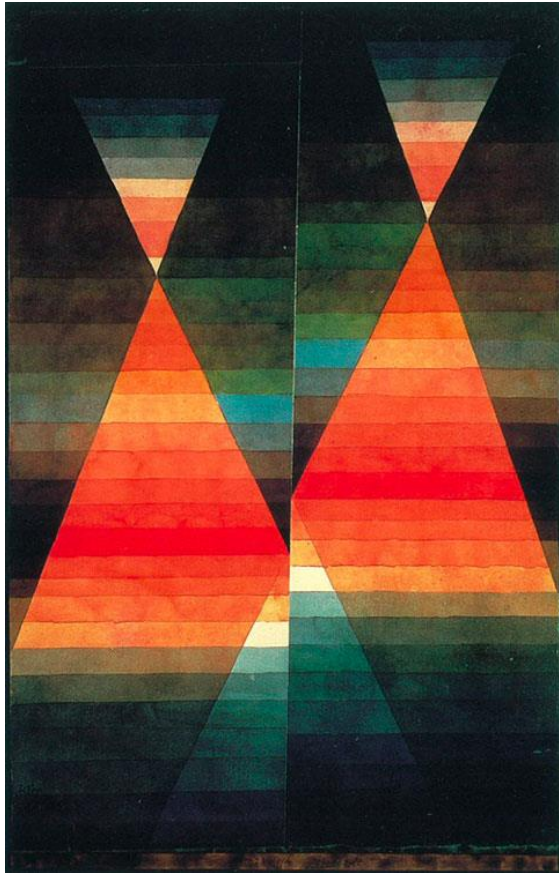


- **explorative search for new materials & predictive design**
- **high quality single crystal growth**
- **epitaxial growth** of ultrathin films and heterostructures
- **2D materials and micro/nano structures**



the materials

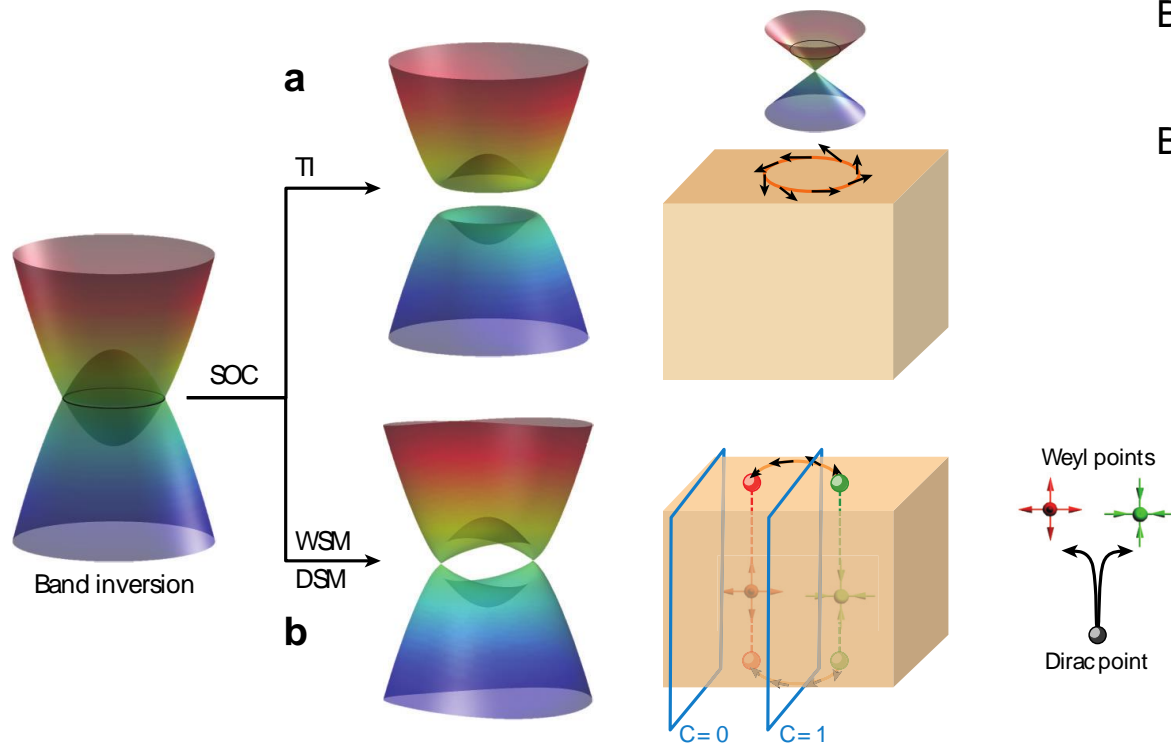




Weyl semimetals

Breaking time reversal symmetry

Weyl semimetals

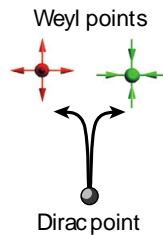
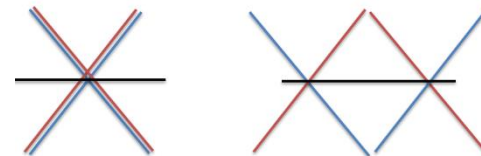


Breaking symmetry

- Inversion symmetry (Strain)

Breaking time reversal symmetry

- Magnetic field

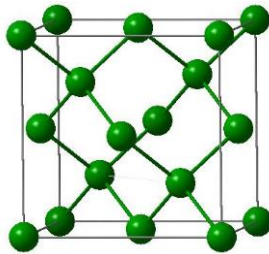


- Dirac points at high symmetry
- Weyl points at low symmetry
- **All crossings in ferromagnets: Weyl points**

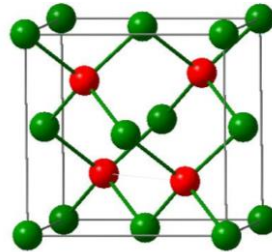


the Heusler family

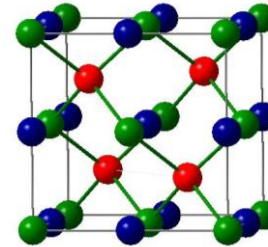
Diamond



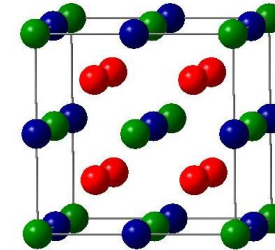
ZnS



Heusler XYZ C1_b



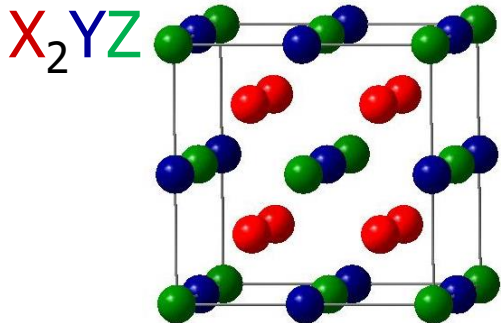
X₂YZ L2₁



C 2.55	N 3.04
Si 1.90	P 2.19
Ge 2.01	As 2.18
Sn 1.96	Sb 2.05

H 2.20																	He	
Li 0.98	Be 1.57											B 2.04	C 2.55	N 3.04	O 3.44	F 3.98	Ne	
Na 0.93	Mg 1.31											Al 1.61	Si 1.90	P 2.19	S 2.58	Cl 3.16	Ar	
K 0.82	Ca 1.00	Sc 1.36	Ti 1.54	V 1.63	Cr 1.66	Mn 1.55	Fe 1.83	Co 1.88	Ni 1.91	Cu 1.90	Zn 1.65	Ga 1.81	Ge 2.01	As 2.18	Se 2.55	Br 2.96	Kr 3.00	
Rb 0.82	Sr 0.95	Y 1.22	Zr 1.33	Nb 1.60	Mo 2.16	Tc 1.90	Ru 2.20	Rh 2.28	Pd 2.20	Ag 1.93	Cd 1.69	In 1.78	Sn 1.96	Sb 2.05	Te 2.10	I 2.66	Xe 2.60	
Cs 0.79	Ba 0.89			Hf 1.30	Ta 1.50	W 1.70	Re 1.90	Os 2.20	Ir 2.20	Pt 2.20	Au 2.40	Hg 1.90	Tl 1.80	Pb 1.80	Bi 1.90	Po 2.00	At 2.20	Rn
Fr 0.70	Ra 0.90																	
		La 1.10	Ce 1.12	Pr 1.13	Nd 1.14	Pm 1.13	Sm 1.17	Eu 1.20	Gd 1.20	Tb 1.10	Dy 1.22	Ho 1.23	Er 1.24	Tm 1.25	Yb 1.10	Lu 1.27		
		Ac 1.10	Th 1.30	Pa 1.50	U 1.70	Np 1.30	Pu 1.28	Am 1.13	Cm 1.28	Bk 1.30	Cf 1.30	Es 1.30	Fm 1.30	Md 1.30	No 1.30	Lr 1.30		

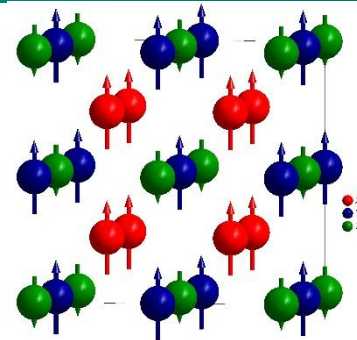
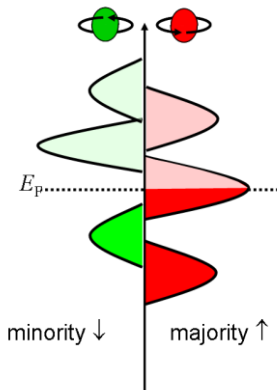
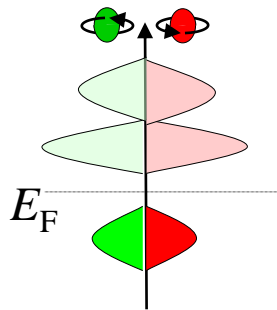
from semiconductors to half metals



- magic valence electron number: 24
- valence electrons = 24 + magnetic moments



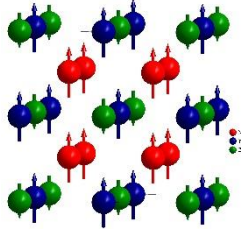
$$2 * 8 + 5 + 3 = 24$$



$$2 * 9 + 7 + 3 = 24 + 4$$



tuning exchange



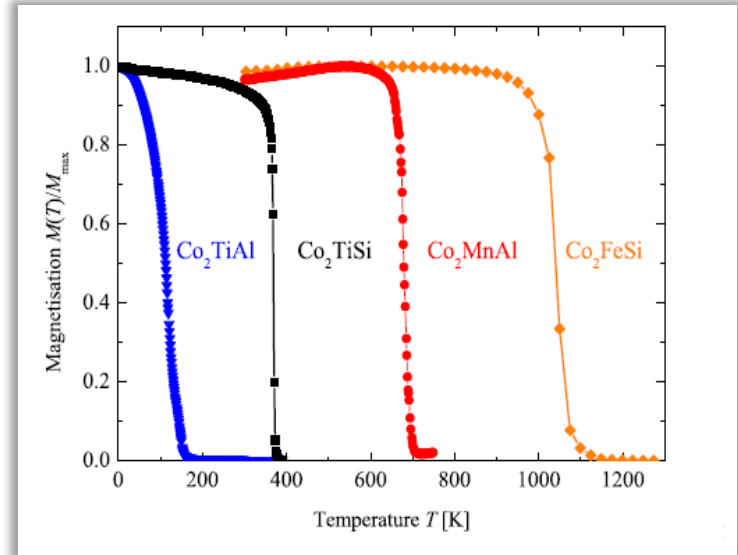
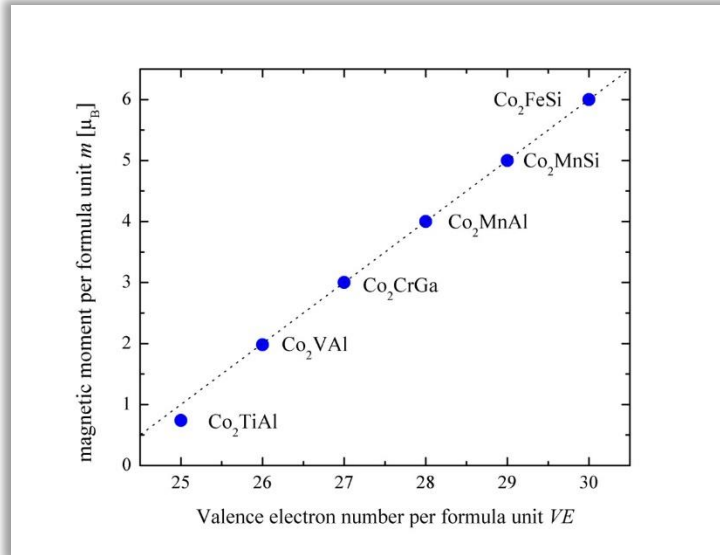
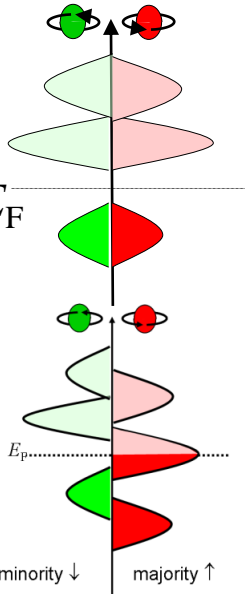
$$\text{Co}_2\text{TiAl}: 2 \times 9 + 4 + 3 = 25 \quad M_s = 1m_B$$



$$\text{Co}_2\text{MnGa}: 2 \times 9 + 7 + 3 = 28 \quad M_s = 4m_B$$



$$\text{Co}_2\text{FeSi}: 2 \times 9 + 8 + 4 = 30 \quad M_s = 6m_B$$



Kübler *et al.*, PRB **28**, 1745 (1983)
 de Groot RA, et al. PRL **50** 2024 (1983)
 Galanakis *et al.*, PRB **66**, 012406 (2002)

Kandpal *et al.*, J. Phys. D **40** (2007) 1507
 Balke *et al.* Solid State Com. **150** (2010) 529
 Kübler *et al.*, Phys. Rev. B **76** (2007) 024414

Heusler and Weyl

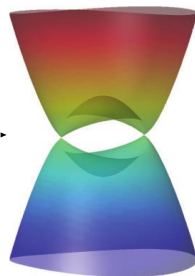


Breaking symmetry

- Inversion symmetry (Strain)

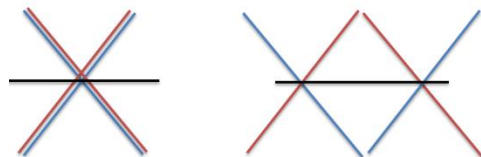
Breaking time reversal symmetry

- Magnetic field

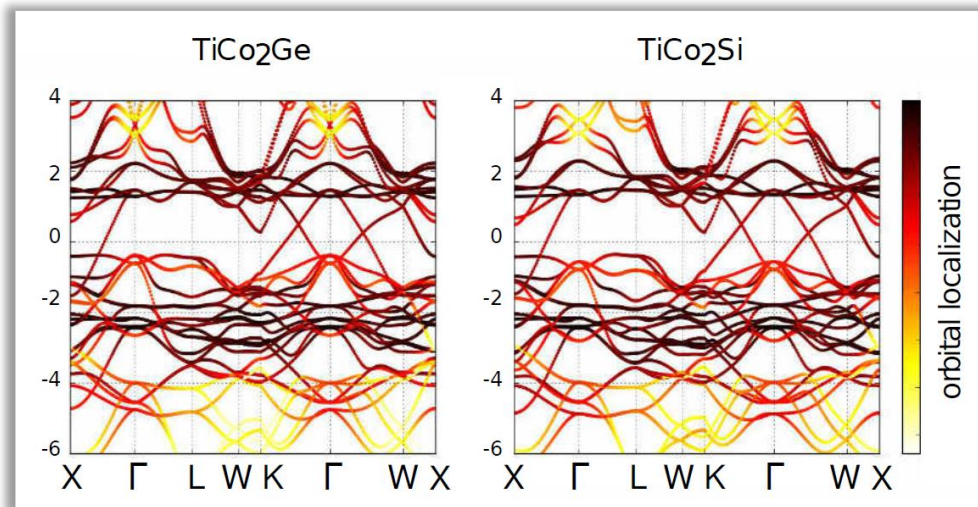


Co₂TiSn

$$\text{Co}_2\text{TiSi: } 2 \times 9 + 4 + 4 = 26 \quad M_s = 2\mu_B$$



- Dirac points at high symmetry
- Weyl points at low symmetry
- All crossings in **ferromagnets**:
Weyl points



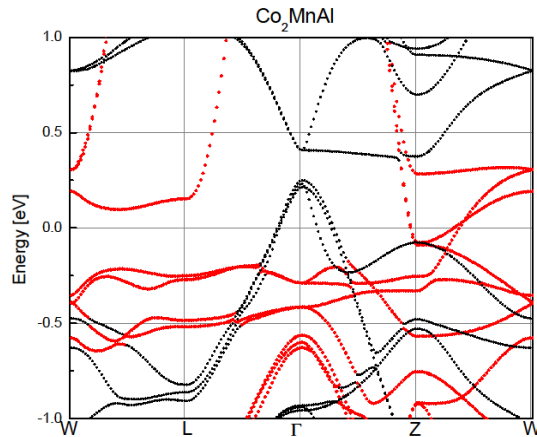
Heusler, Weyl and Berry



Giant AHE in Co₂MnAl

$\sigma_{xy} = 1800 \text{ S/cm}$ calc.

$\sigma_{xy} \approx 2000 \text{ S/cm}$ meas.



$$\sigma_{xy}^A(\mu) = ie^2 \left(\frac{1}{2\pi}\right)^3 \int_k dk \sum_{E(n,k) < \mu} f(n,k,\mu) \Omega_{n,xy}(k),$$

Compound ^a	N_V	a (nm)	M^{exp}	M^{calc}	σ_{xy}	P (%)
Co ₂ VGa	26	0.5779	1.92	1.953	66	65
Co ₂ CrAl	27	0.5727	1.7	2.998	438	100
Co ₂ VSn	27	0.5960	1.21	1.778	-1489	35
Co ₂ MnAl	28	0.5749	4.04	4.045	1800	75
Rh ₂ MnAl	28	0.6022		4.066	1500	94
Mn ₂ PtSn ^b	28	0.4509 (1.3477)		6.66	1108	91
Co ₂ MnSn	29	0.5984	5.08	5.00	118	82
Co ₂ MnSi	29	0.5645	4.90	4.98	228	100

$$\rho_{xy}^M = (\alpha \rho_{xx} + \beta \rho_{xx}^2) M. ???$$

Heusler, Weyl and Berry



PHYSICAL REVIEW B 85, 012405 (2012)

Berry curvature and the anomalous Hall effect in Heusler compounds

Jürgen Kübler^{1,*} and Claudia Felser²

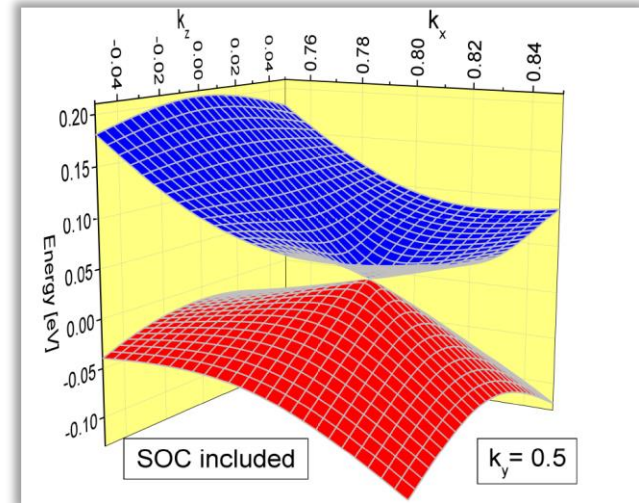
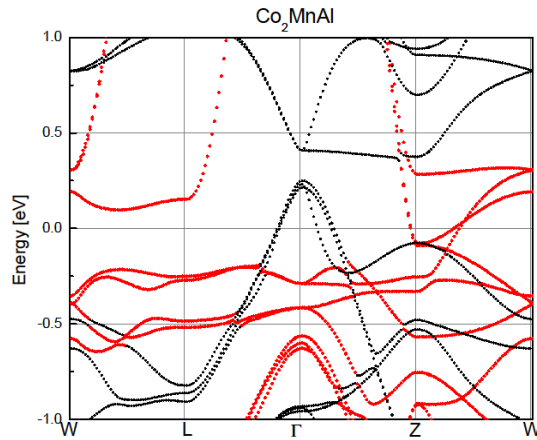
Giant AHE in Co₂MnAl

Co₂MnGa

$\sigma_{xy} = 1800 \text{ S/cm calc.}$

$\sigma_{xy} \approx 2000 \text{ S/cm meas.}$

$$\sigma_{xy}^A(\mu) = ie^2 \left(\frac{1}{2\pi}\right)^3 \int dk \sum_{E(n,k) < \mu} f(n,k,\mu) \Omega_{n,xy}(k),$$

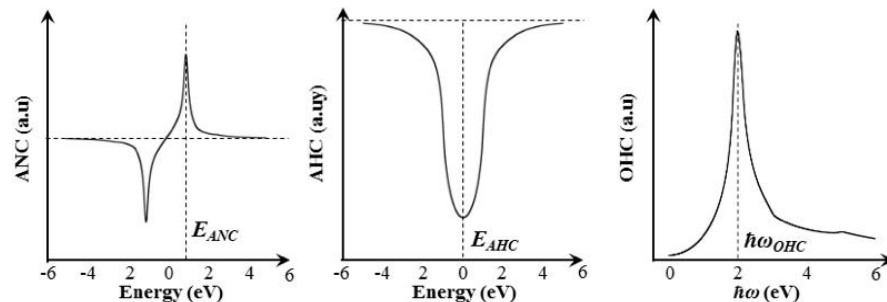
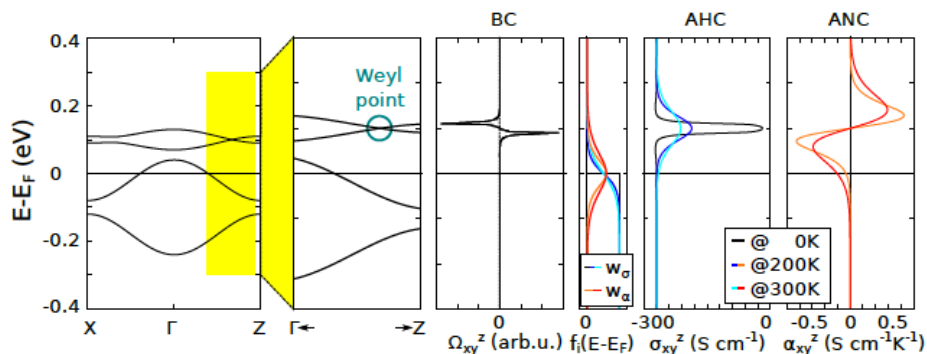
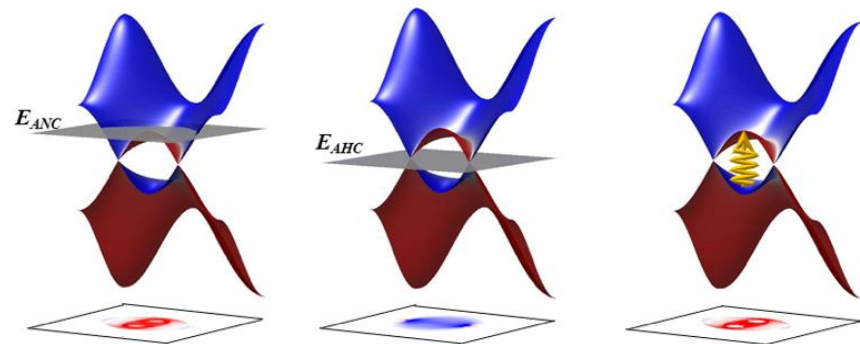
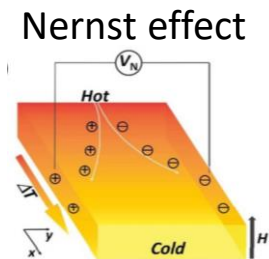




Berry curvature design

Berry curvature design

- giant spin Hall
- giant anomalous Hall
- giant topological Hall
- giant anomalous Nernst

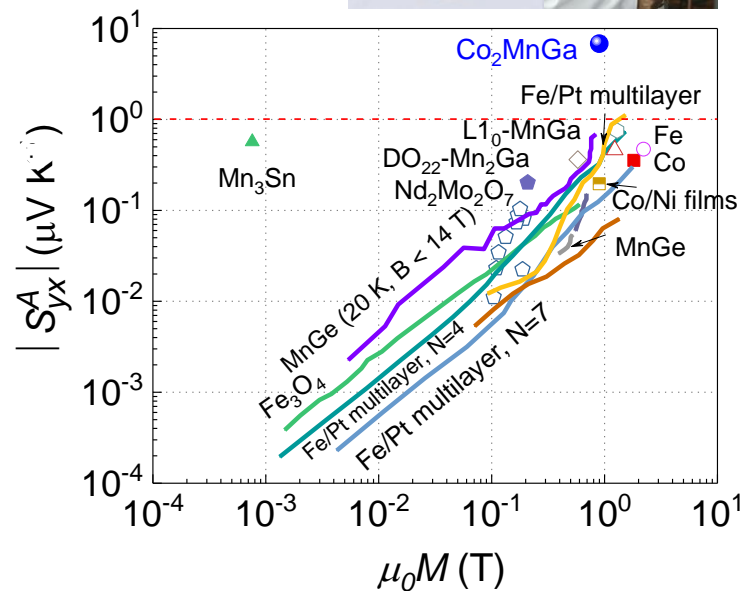
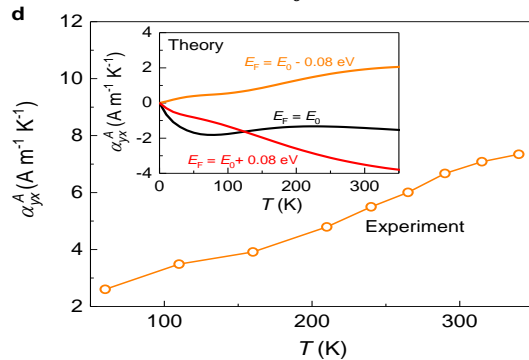
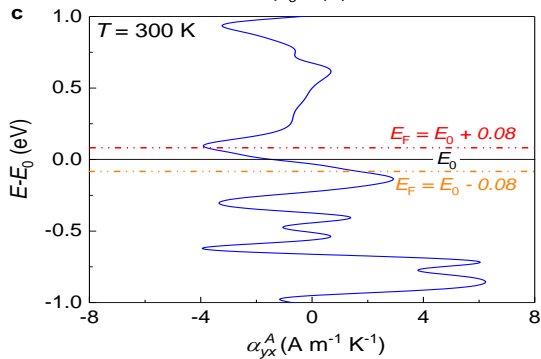
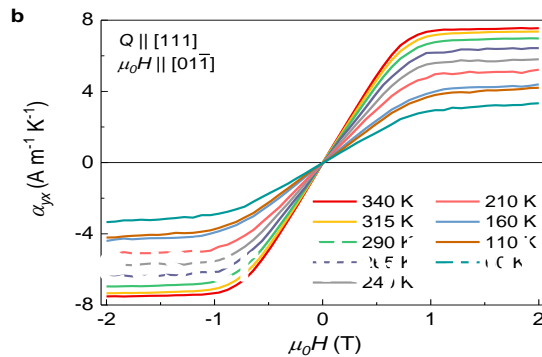
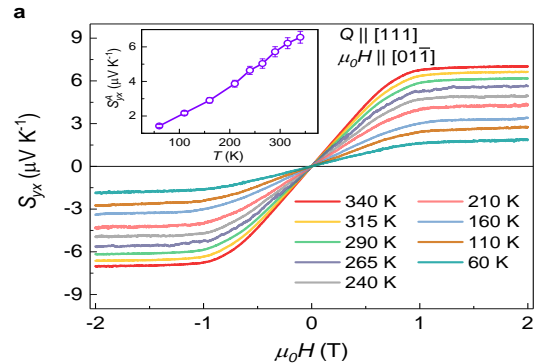


Thermoelectric effect ← Anomalous Hall effect → Magneto-optic effect

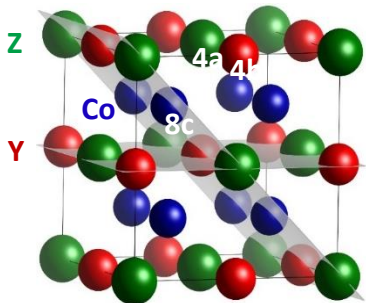
Nernst effect



Co₂MnGa

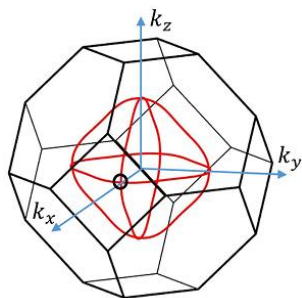
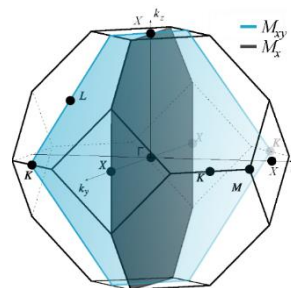


Heusler, Weyl and Berry



Co_2YZ (Y = IVB or VB; Z = IVA or IIIA)

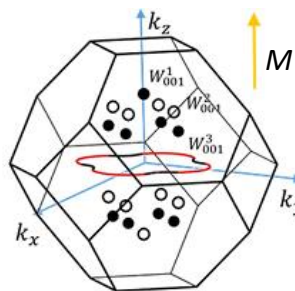
$L2_1$ space group 225 ($Fm\bar{3}m$)



Without SOC

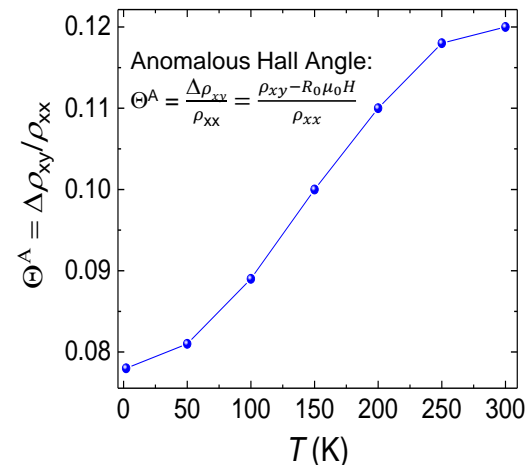
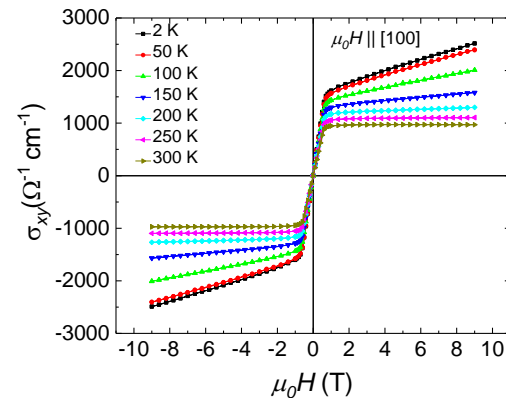
With SOC

Symmetry and electronic structures depend on the magnetization direction



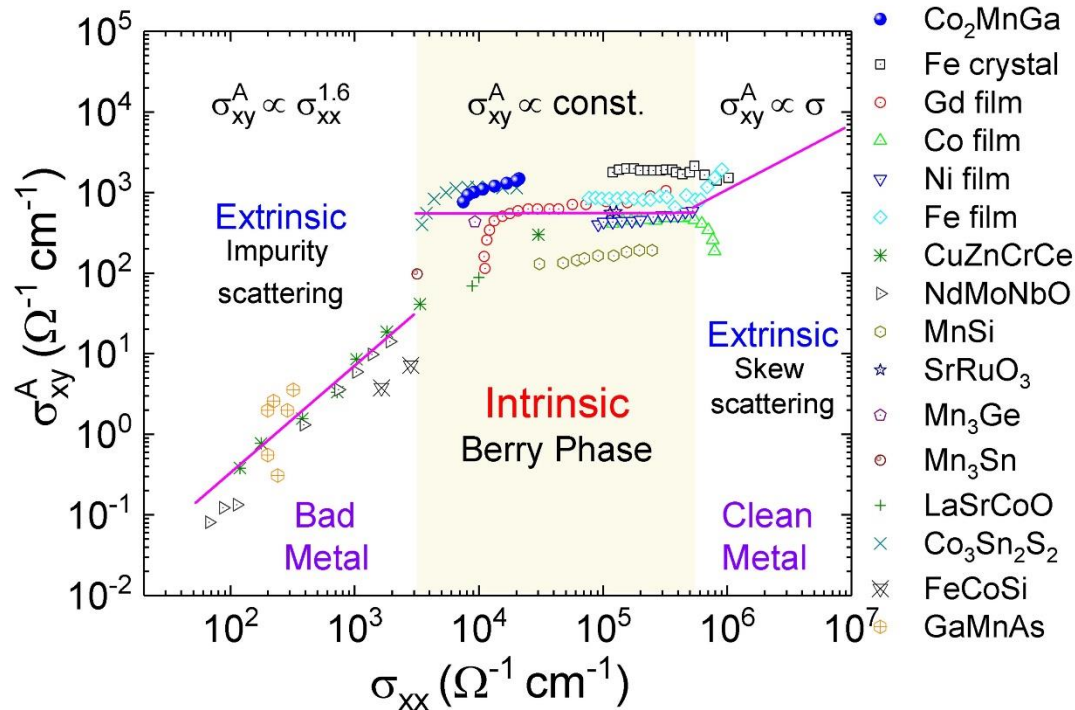
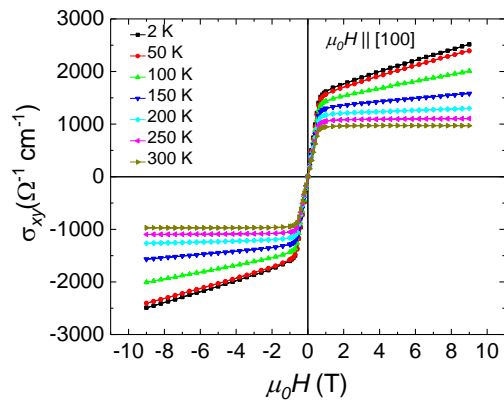
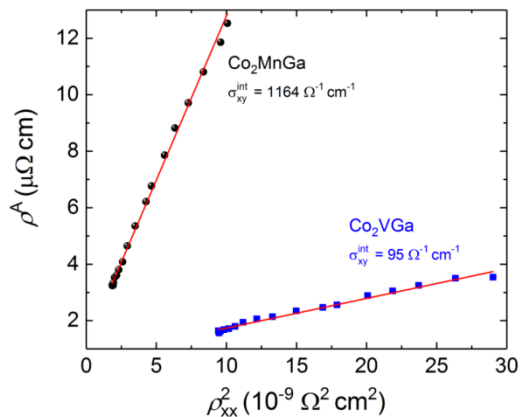
Phys. Rev. Lett. 117, 236401 (2016)

Sci. Rep. 6, 38839 (2016)

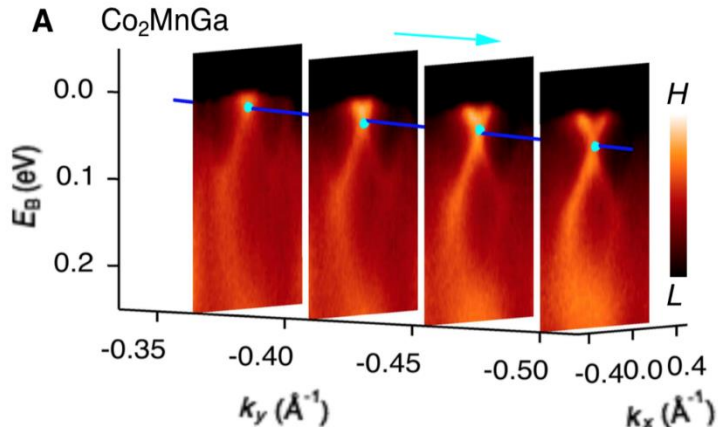
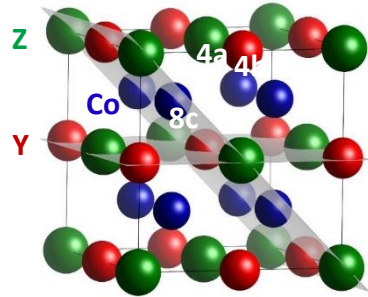


- ❑ nodal line is formed in the plane when bands of opposite mirror eigenvalues cross.
- ❑ Mirror planes are related to each other by the rotations

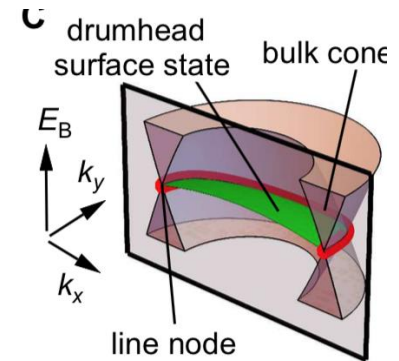
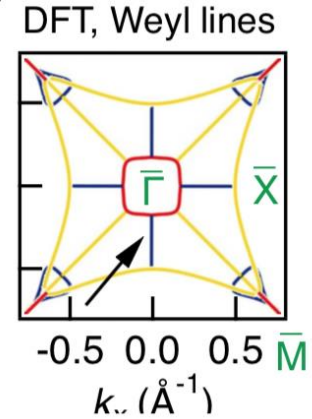
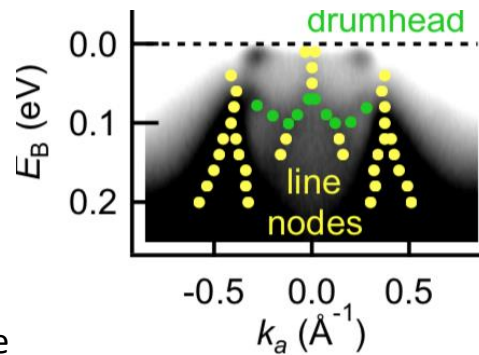
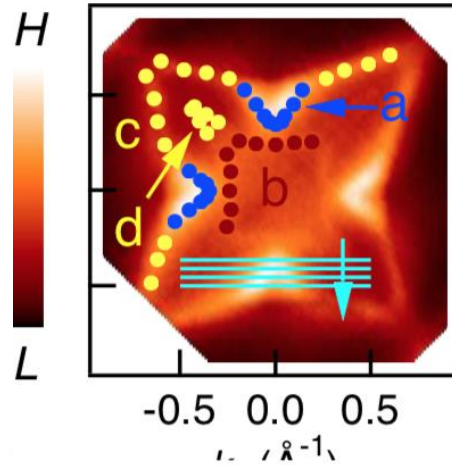
Heusler, Weyl and Berry



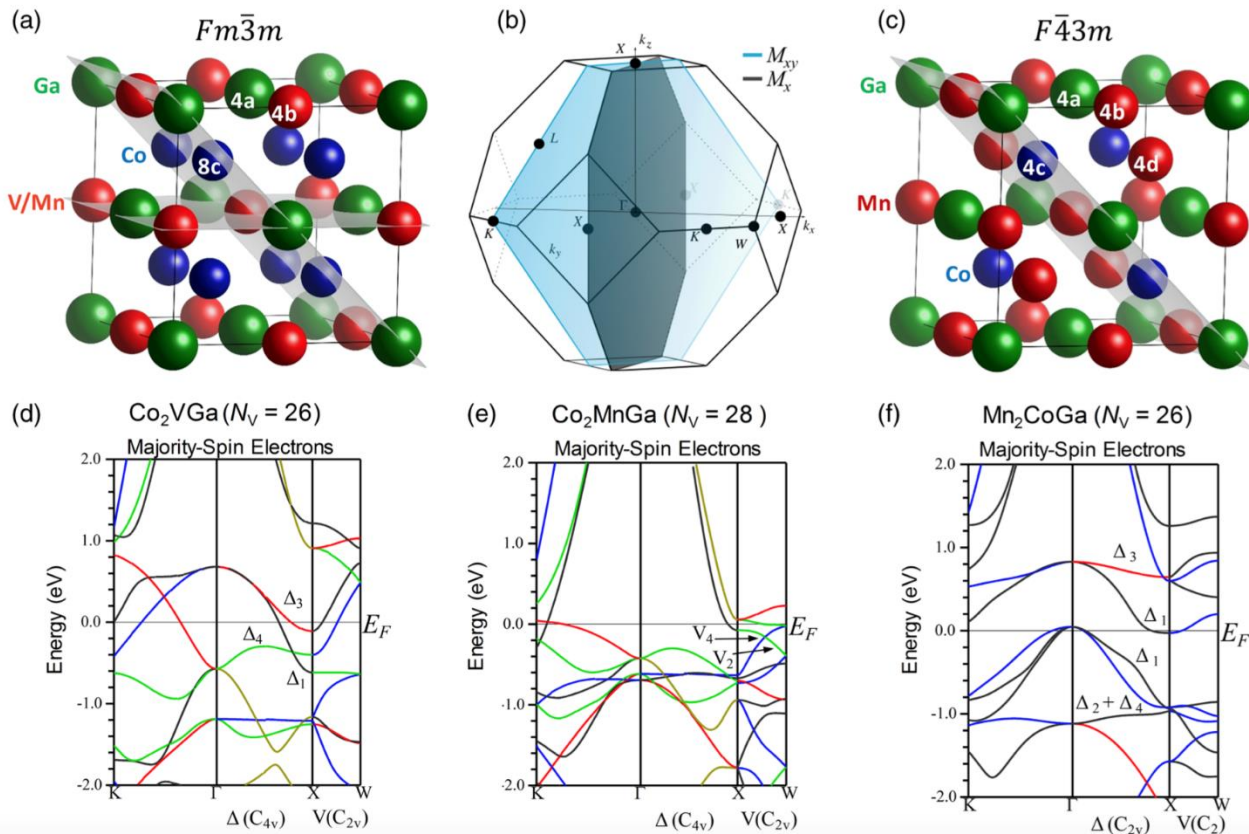
Co₂MnGa – ferromagnetic nodal line



Series of ARPES cuts through the candidate line node

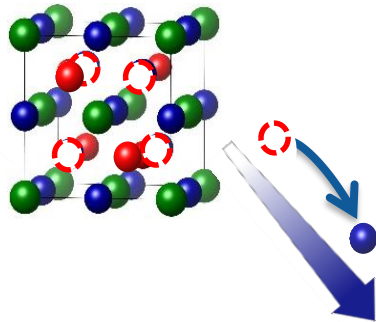


Heusler, Weyl and Berry

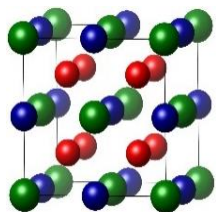




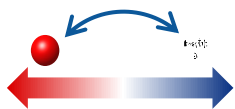
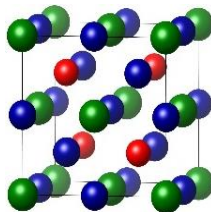
Half-Heusler, $F\bar{4}3m$ (no. 216)



Regular-Heusler, $Fm\bar{3}m$ (no. 225)



Inverse-Heusler, $F\bar{4}3m$ (no. 216)



no inversion symmetry
topology !

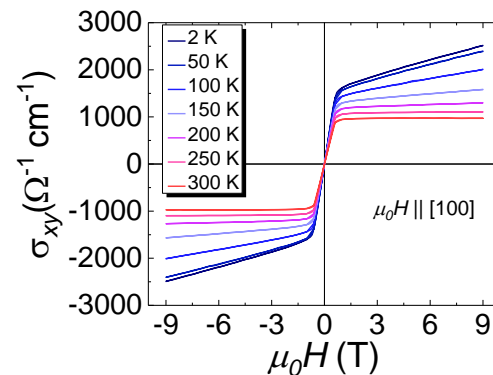
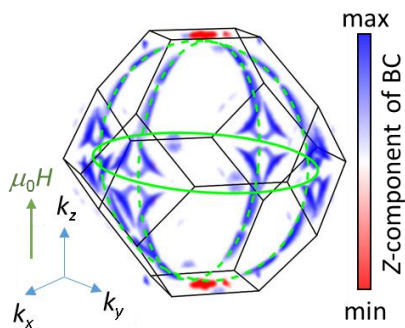
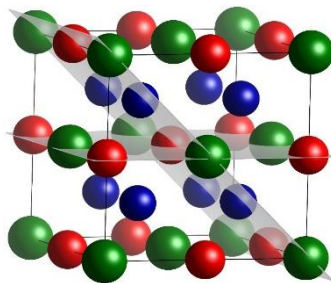


Heusler, Weyl and Berry

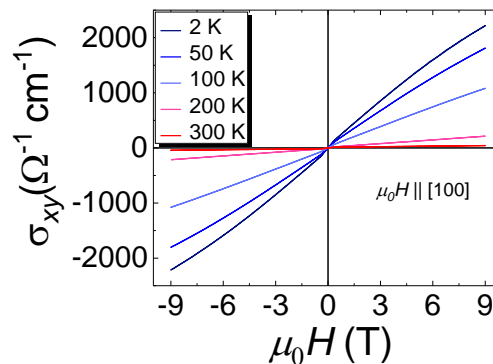
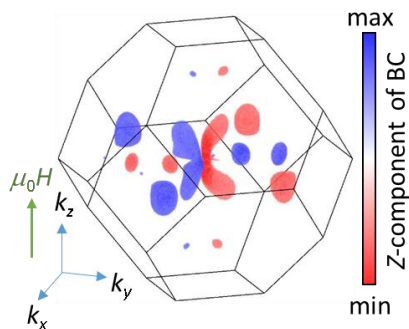
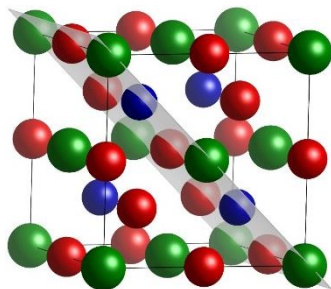


playing with symmetry: from Weyl to spinless semiconductor

Co₂MnGa



Mn₂CoGa

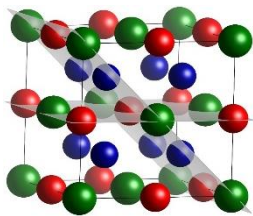


Heusler, Weyl and Berry

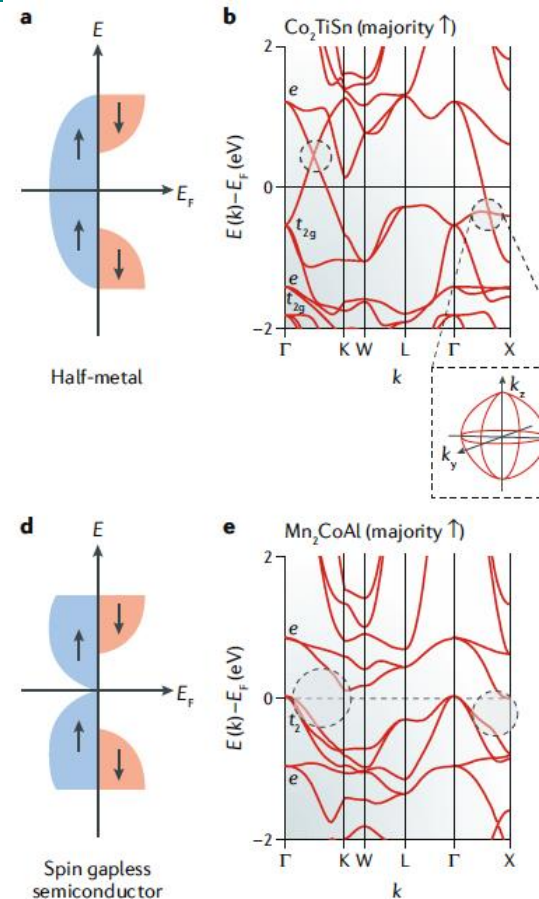
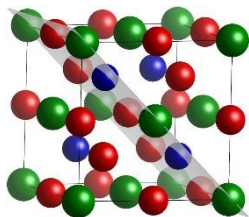


playing with symmetry: from Weyl to spin gapless semiconductor

Co₂TiSn



Mn₂CoGa



Quardi, Fecher, Kübler, and Felser, Physical Review Letter 110 (2013) 100401

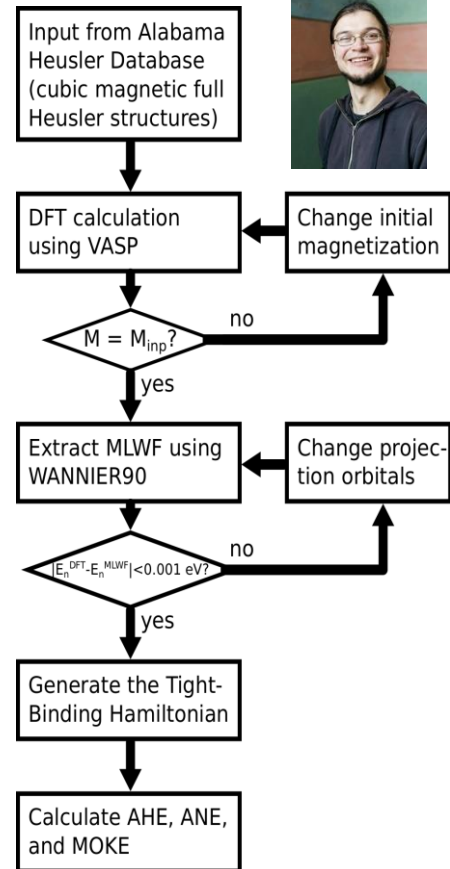
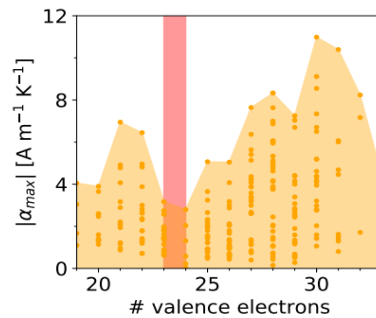
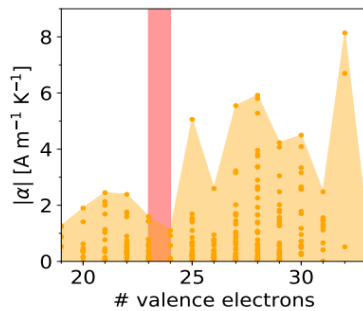
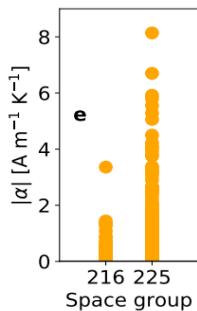
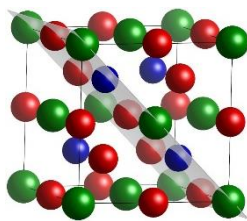
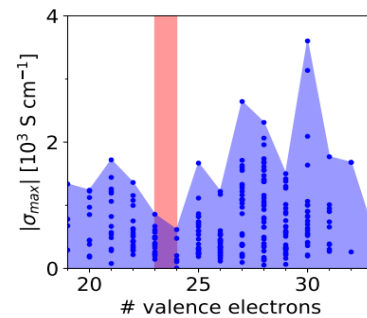
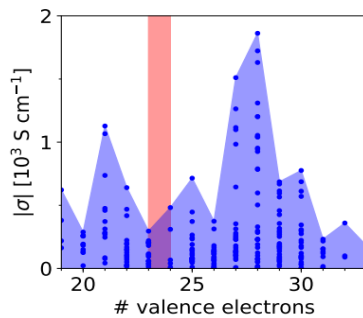
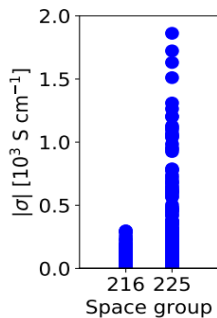
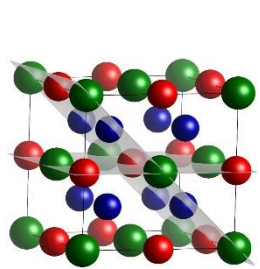
Manna et al., Phys. Rev. X 8 (2018) 041045, arXiv:1712.10174

Manna et al., Nature Review Materials, 3 (2018) 244 arXiv:1802.02838v1

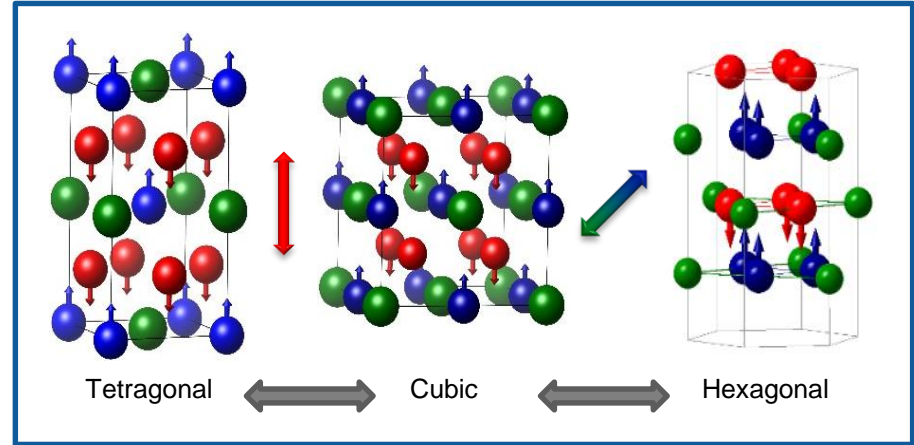
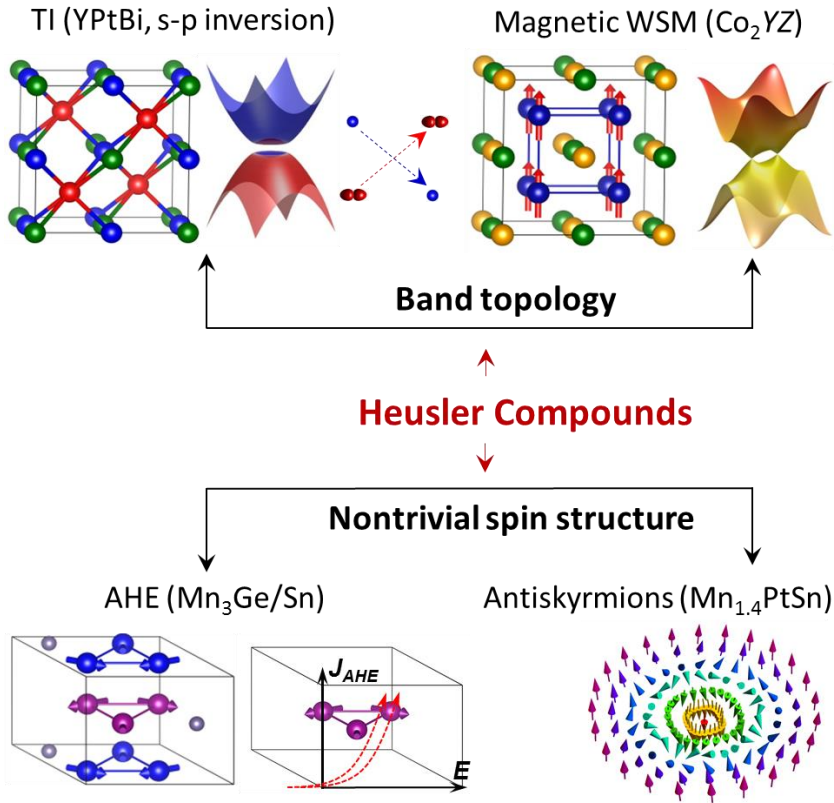
high through put



playing with symmetry:



Heusler, Weyl and Berry



Mn_3Ga Mn_3Ge Mn_3Sn

Heusler, Weyl and Berry



PRL 112, 017205 (2014)

PHYSICAL REVIEW LETTERS

week ending
10 JANUARY 20

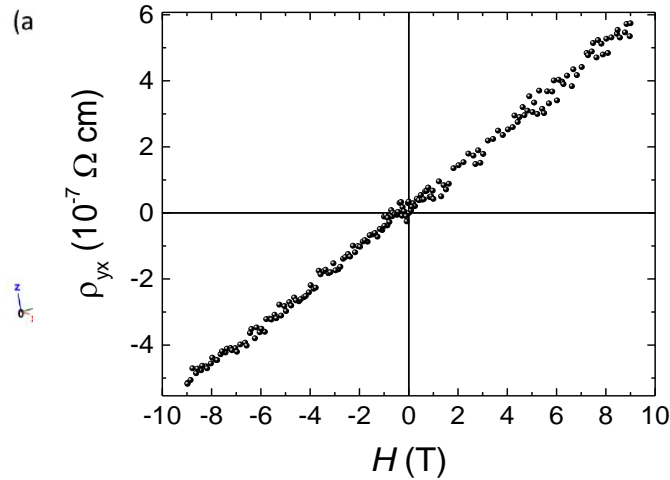
epl A LETTERS JOURNAL EXPLORING
THE FRONTIERS OF PHYSICS

December 2014

www.epljournal.org

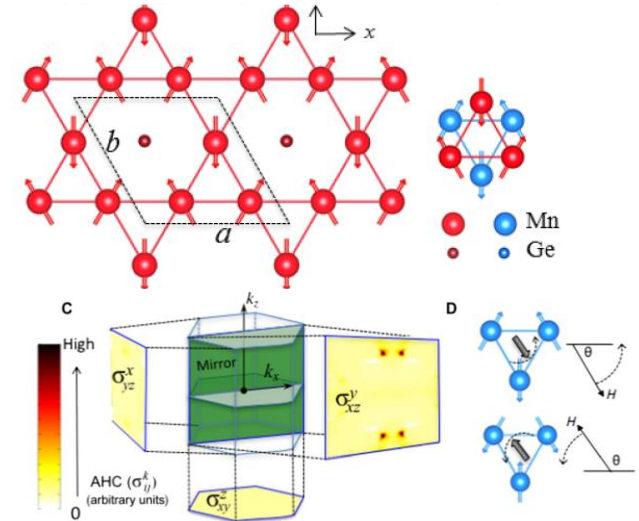
Anomalous Hall Effect Arising from Noncollinear Antiferromagnetism

Hua Chen, Qian Niu, and A. H. MacDonald



Non-collinear antiferromagnets and the anomalous Hall effect

J. KÜBLER¹ and C. FELSER²

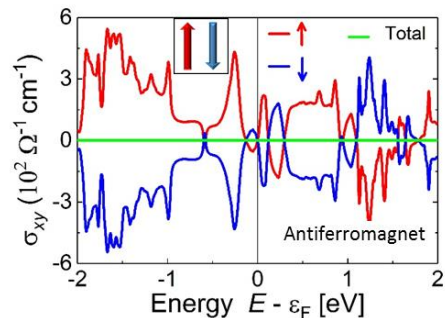
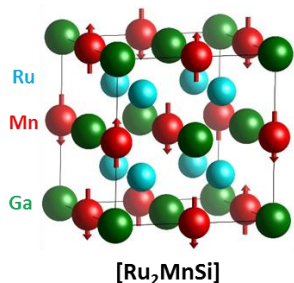


For the planar cases the AHC is connected with Weyl points in the energy- band structure.

Heusler, Weyl and Berry

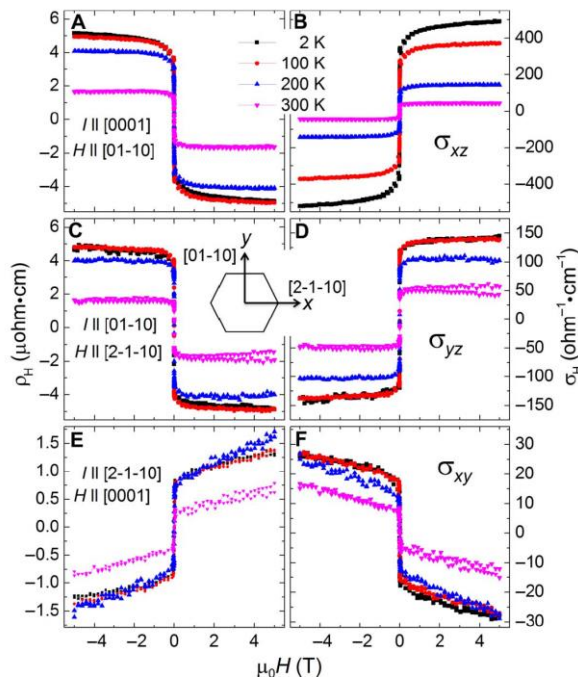


$$\sigma_{xy}^A(\mu) = ie^2 \left(\frac{1}{2\pi}\right)^3 \int_k dk \sum_{E(n,\mathbf{k}) < \mu} f(n,\mathbf{k},\mu) \Omega_{n,xy}(\mathbf{k}),$$



The anomalous Hall conductivity in an antiferromagnetic metal is zero

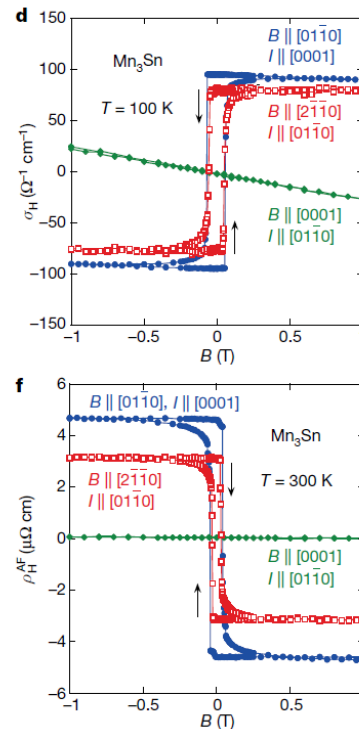
Mn₃Ge
Mn₃Sn



LETTER

Large anomalous Hall effect in a non-collinear antiferromagnet at room temperature

Satoru Nakatsuji¹, Naoki Kiyohara¹ & Tomoya Higo¹



Nayak et al. arXiv:1511.03128, Science Advances 2 (2016) e1501870

Kiyohara, Nakatsuji, preprint: arXiv:1511.04619

Nakatsuji, Kiyohara, & Higo, Nature, doi:10.1038/nature15723

Nernst effect in Mn_3Sn



PRL 119, 056601 (2017)

PHYSICAL REVIEW LETTERS

week ending
4 AUGUST 2017

nature
physics

LETTERS

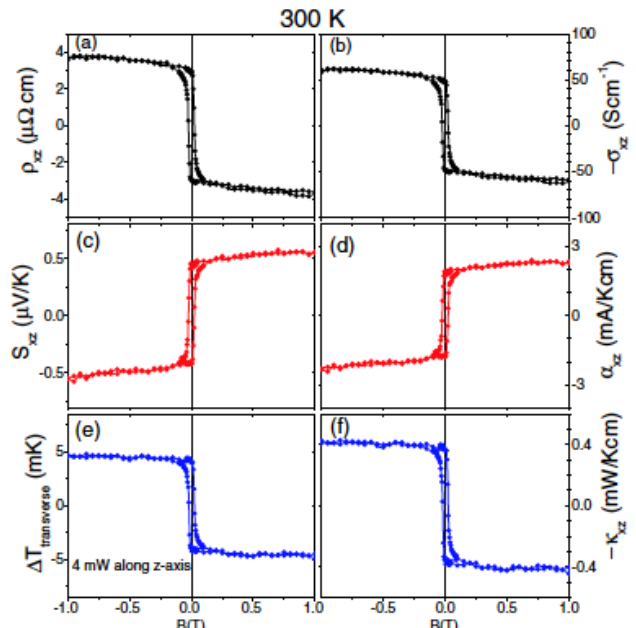
PUBLISHED ONLINE: 24 JULY 2017 | DOI: 10.1038/NPHYS4181

Anomalous Nernst and Righi-Leduc Effects in Mn_3Sn : Berry Curvature and Entropy Flow

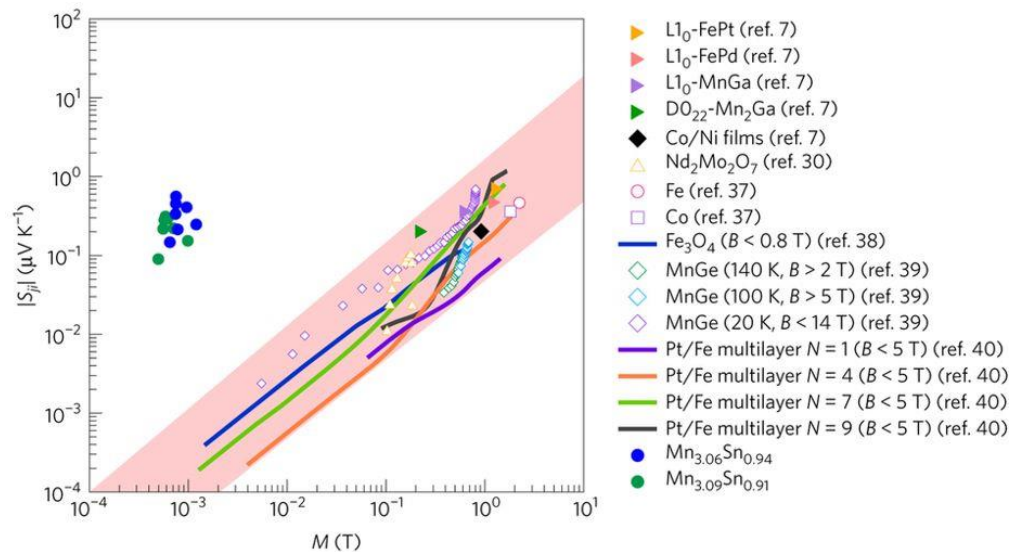
Xiaokang Li,¹ Liangcai Xu,¹ Linchao Ding,¹ Jinhua Wang,¹ Mingsong Shen,¹
Yinfang Lu,¹ Zhenwei Zhu,^{1,2} and Kamran Behnia^{1,2,†}

Large anomalous Nernst effect at room temperature in a chiral antiferromagnet

Muhammad Ikhlas³, Takahiro Tomita³, Takashi Koretsune^{2,3}, Michi-To Suzuki²,
Daisuke Nishio-Hamane¹, Ryotaro Arita^{2,4}, Yoshichika Otani^{1,2,4} and Satoru Nakatsuji^{1,4*}

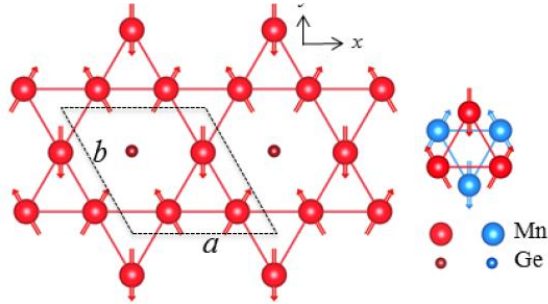


a) Hall resistivity, ρ_{xz} ; (b) Hall conductivity, σ_{xz} , extracted from ρ_{xz} , ρ_{xx} , and ρ_{zz} ; (c) Nernst signal, S_{xz} ; (d) Transverse thermoelectric conductivity, α_{xz} ,

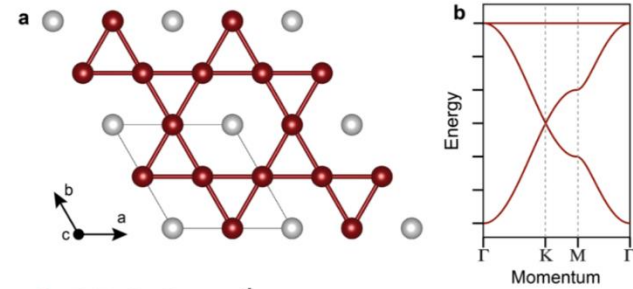


Magnetization dependence of the spontaneous Nernst effect for ferromagnetic metals and Mn_3Sn

Kagome lattice



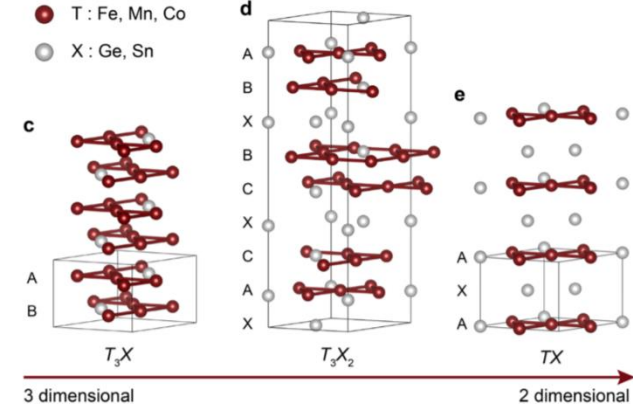
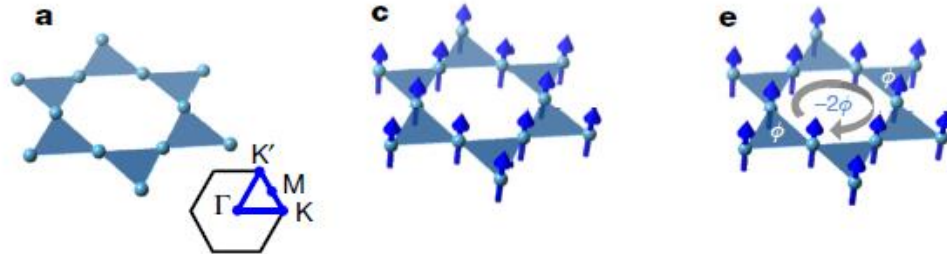
Mn, Fe, Co



LETTER

doi:10.1038/nature25987

Massive Dirac fermions in a ferromagnetic kagome metal



Kagome lattice



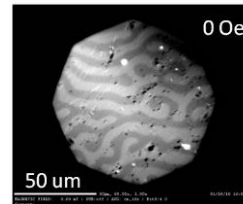
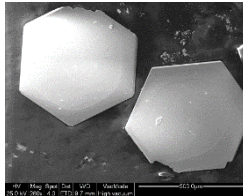
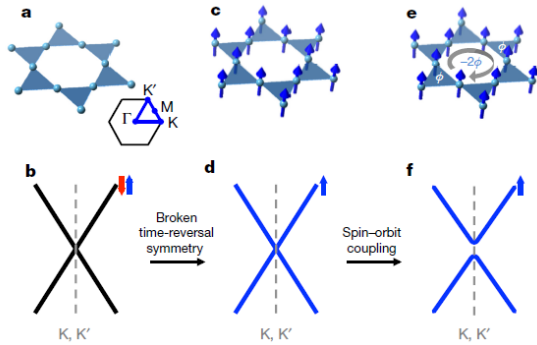
LETTER

doi:10.1038/nature25987

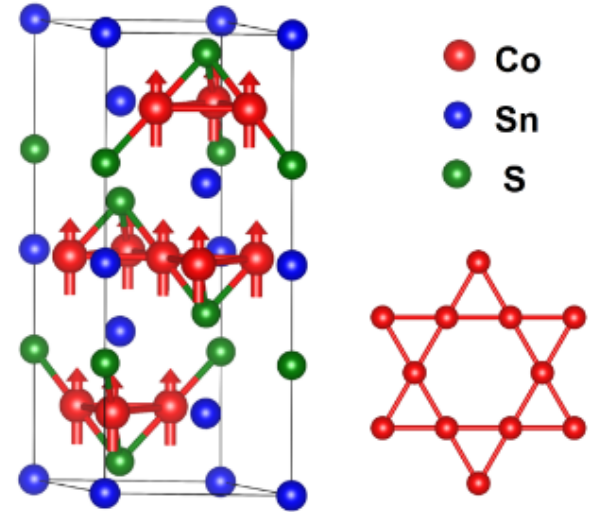
Massive Dirac fermions in a ferromagnetic kagome metal

Fe_3Sn_2

$\text{Co}_3\text{Sn}_2\text{S}_2$

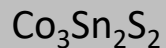
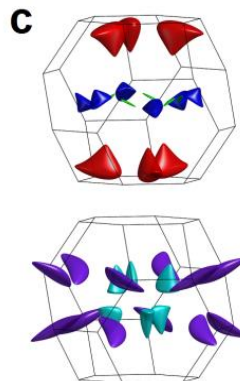
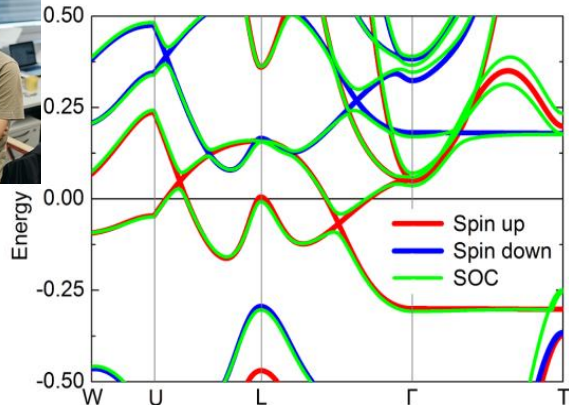


Looking for Weyl fermions on a ferromagnetic Kagomé lattice with out of plane magnetisation.



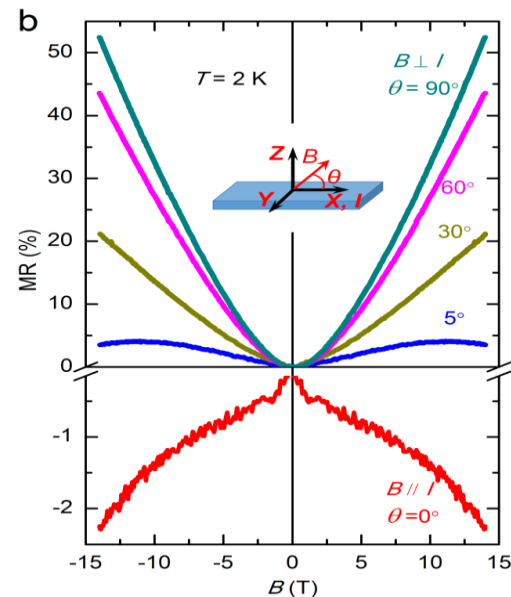
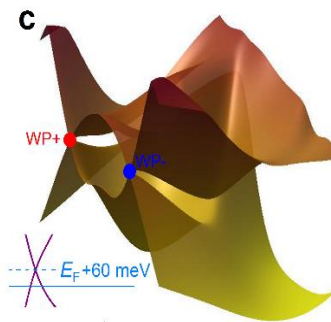
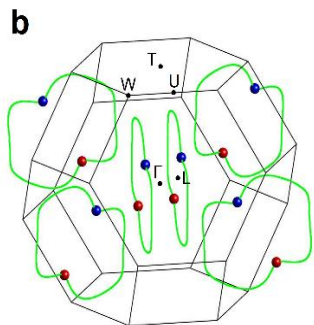
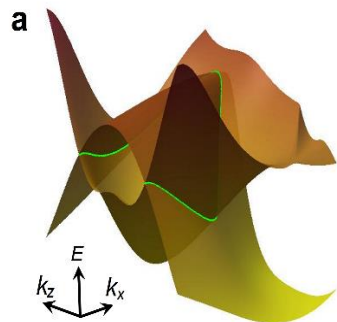


Weyl and Berry



Weyl points are close to EF
Hard magnetic behaviour

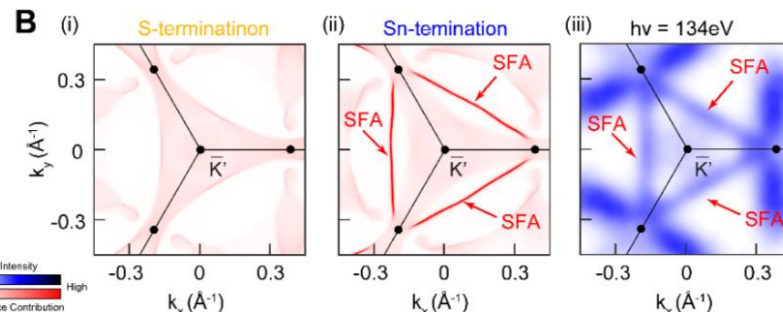
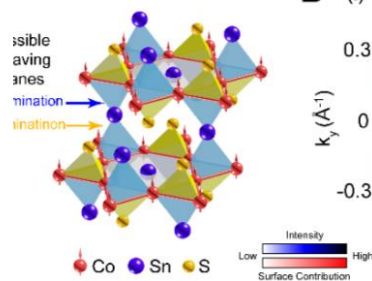
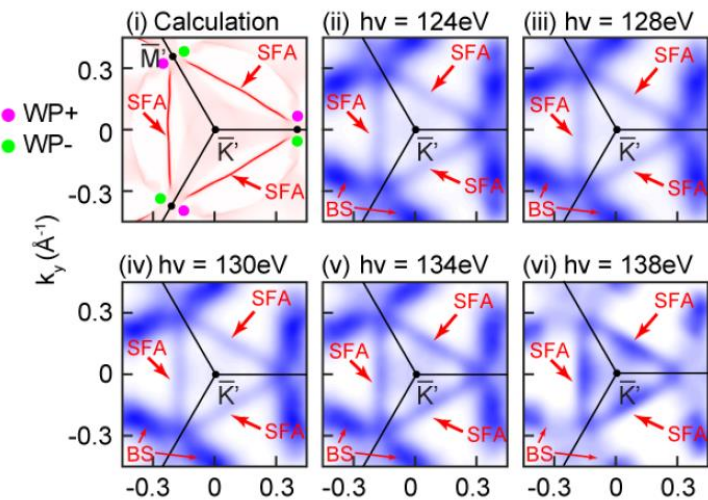
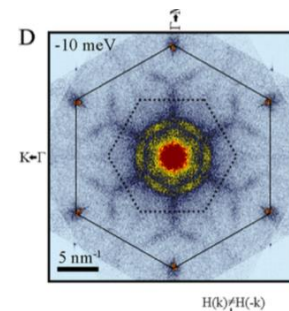
transport: chiral anomaly



Weyl and Berry



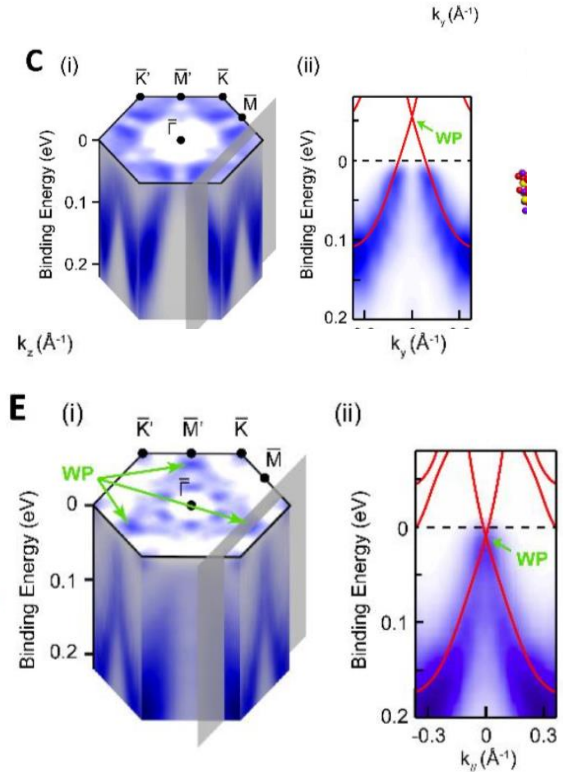
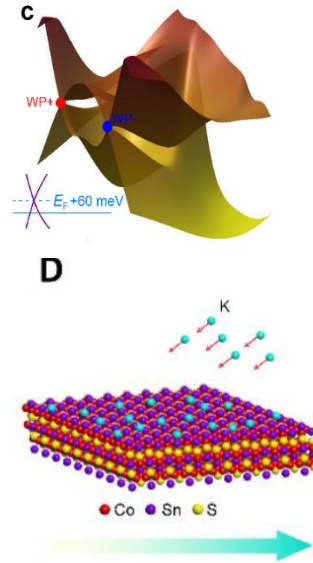
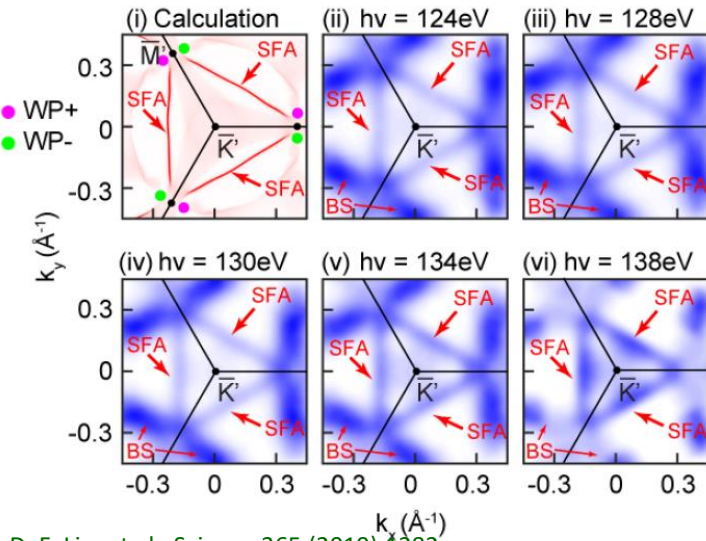
STM and ARPES confirms Weyl and Fermi arcs



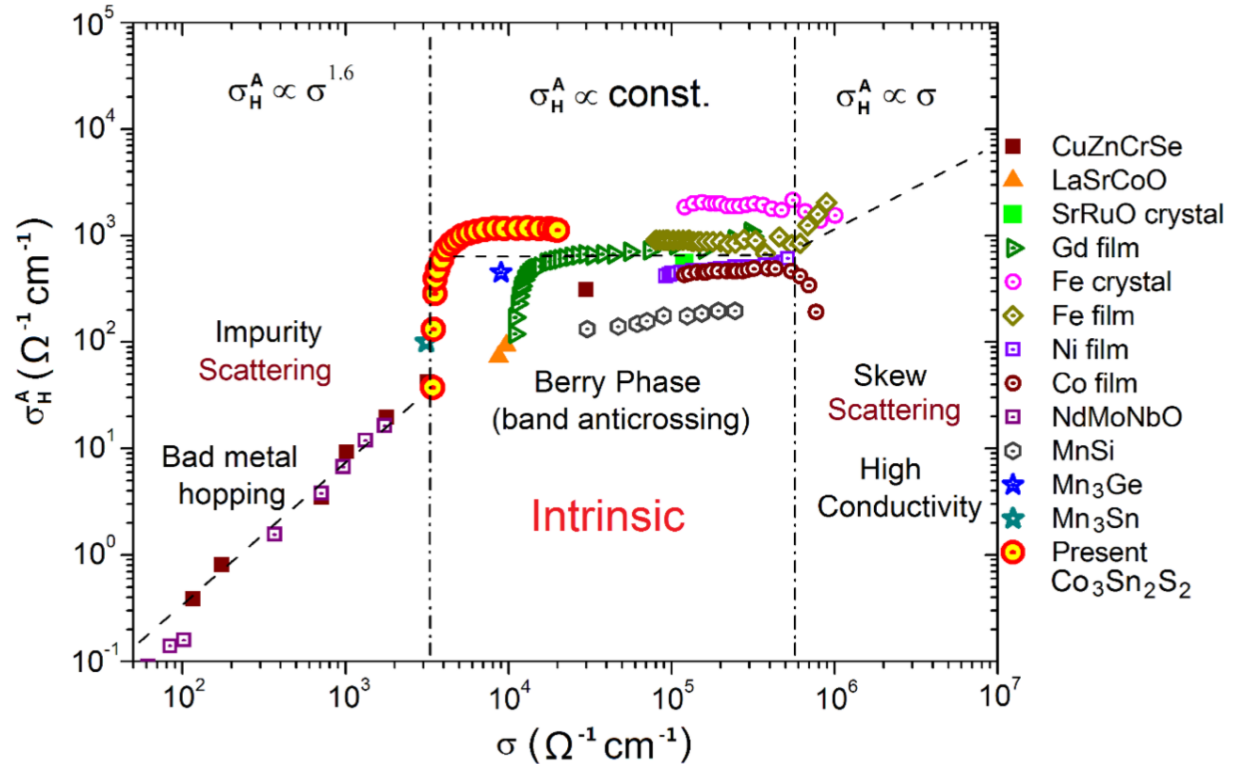
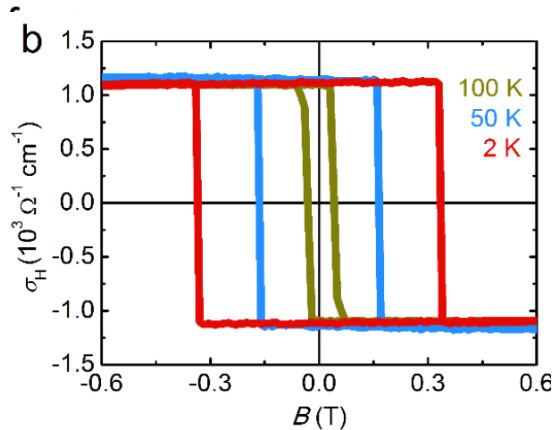
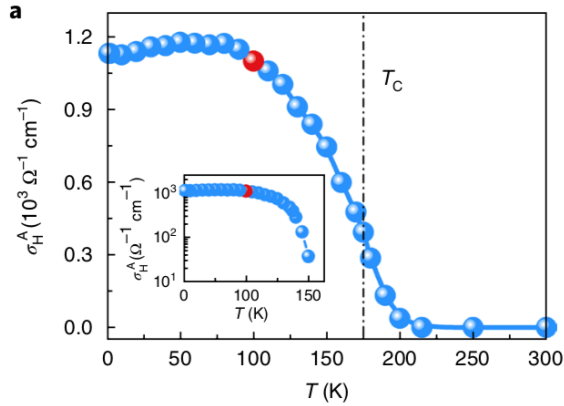
Weyl and Berry



STM and ARPES confirms Weyl and Fermi arcs



new transport properties





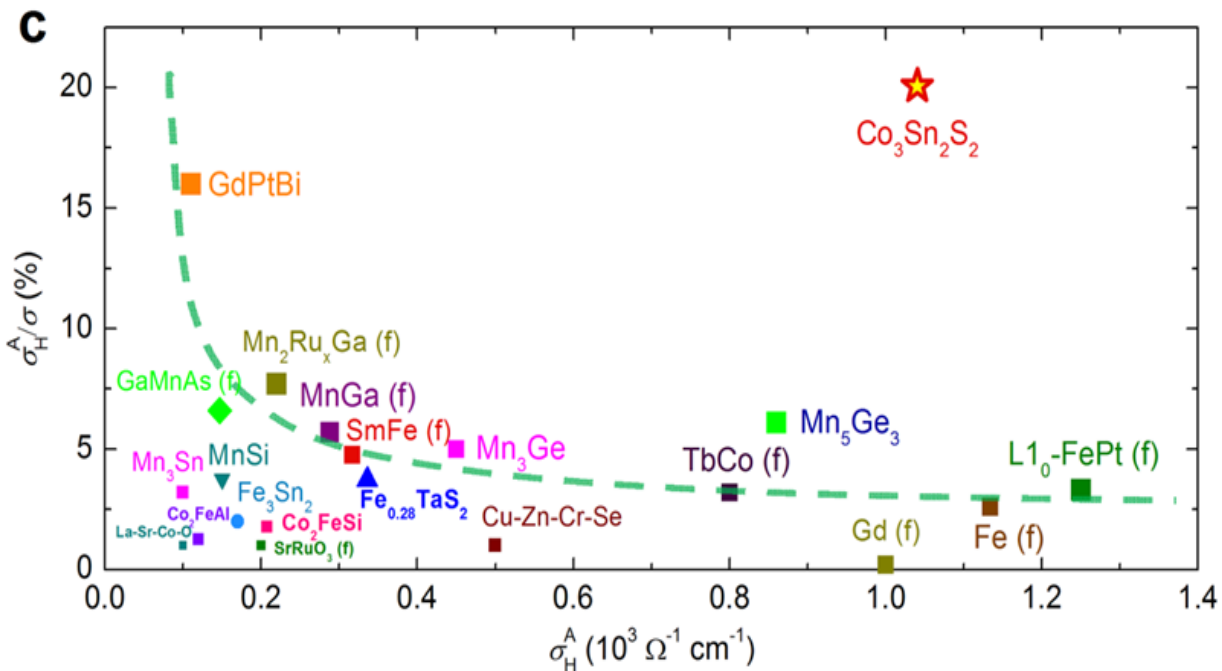
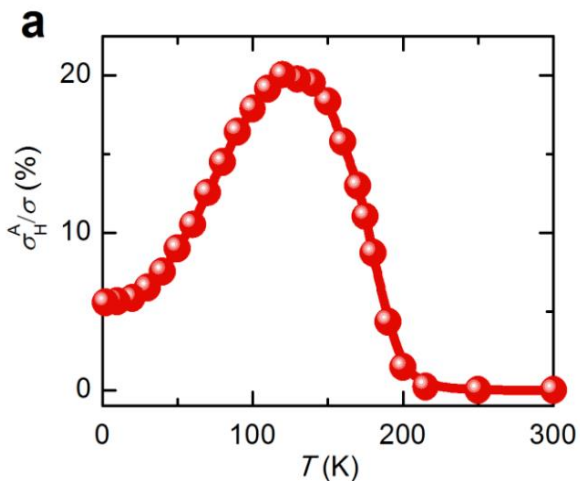
new transport properties

Berry curvature design

- giant anomalous Hall
- giant anomalous Nernst

$\text{Co}_3\text{Sn}_2\text{S}_2$
 Mn_3Sn

Giant Hall Angle 20%



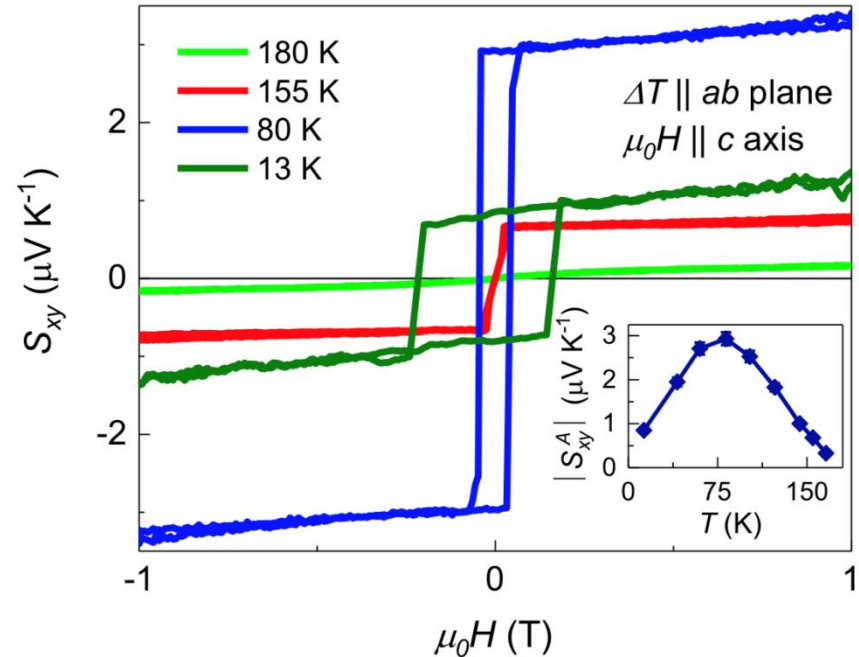
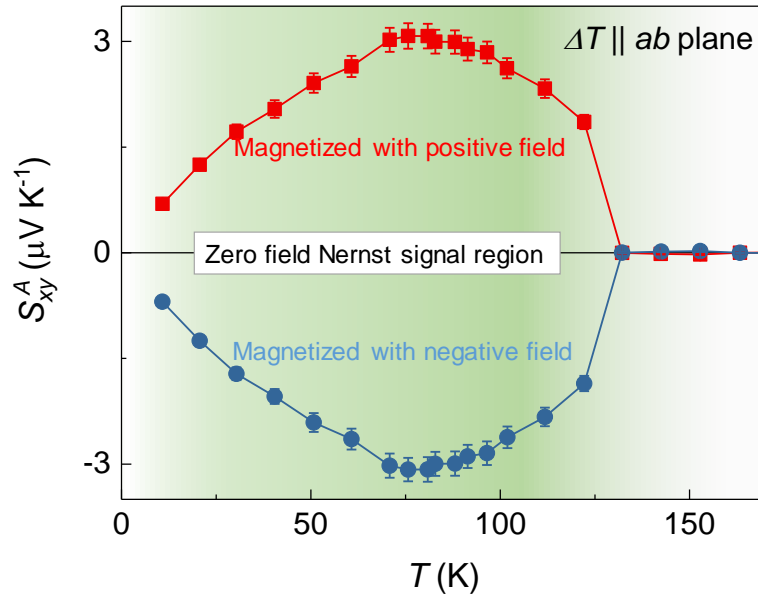
new transport properties



Berry curvature design

- giant anomalous Hall
- giant anomalous Nernst

Co₂MnGa
Co₃Sn₂S₂
Mn₃Sn



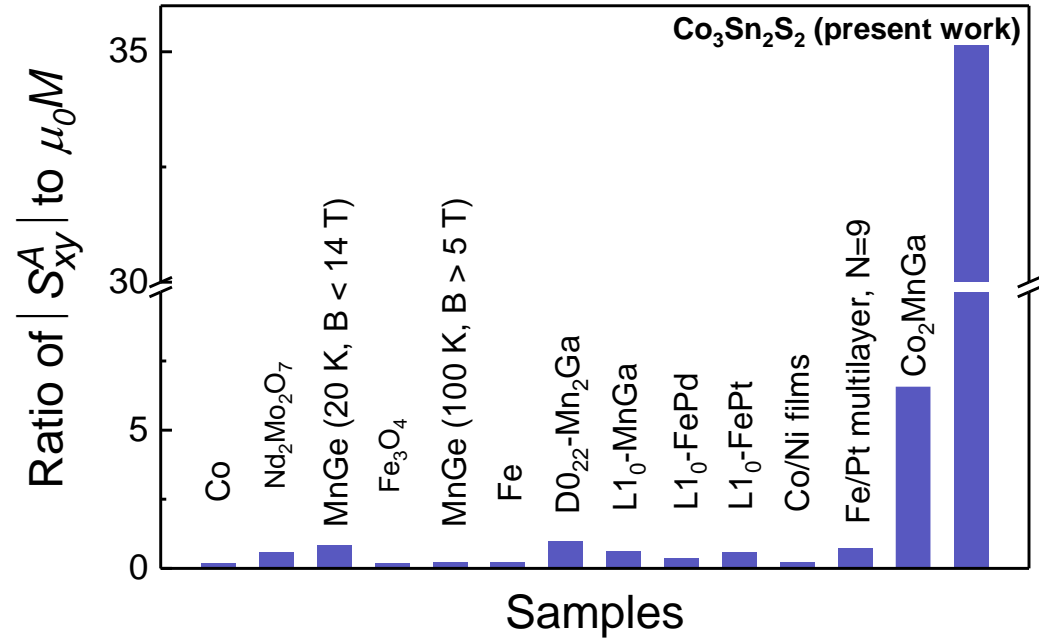
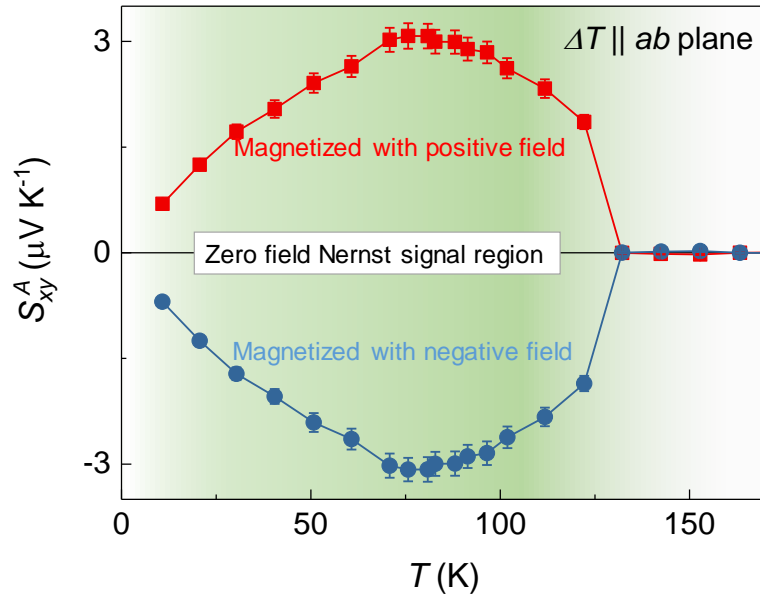
new transport properties



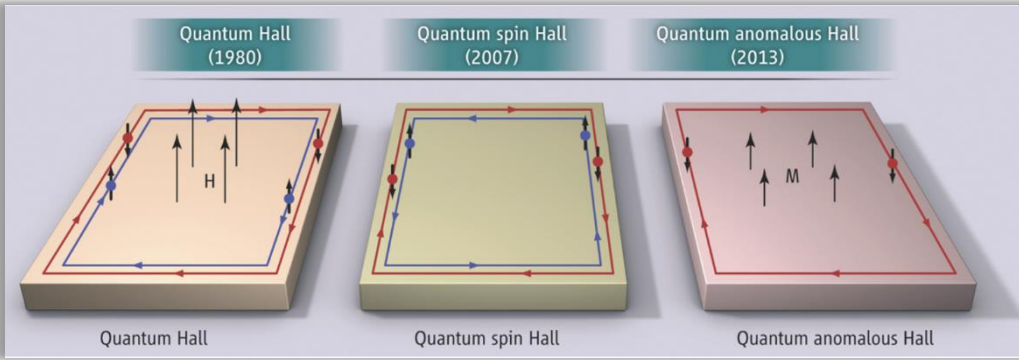
Berry curvature design

- giant anomalous Hall
- giant anomalous Nernst

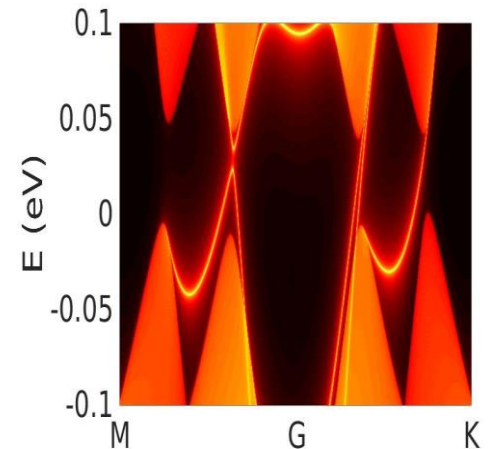
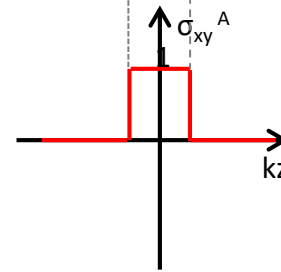
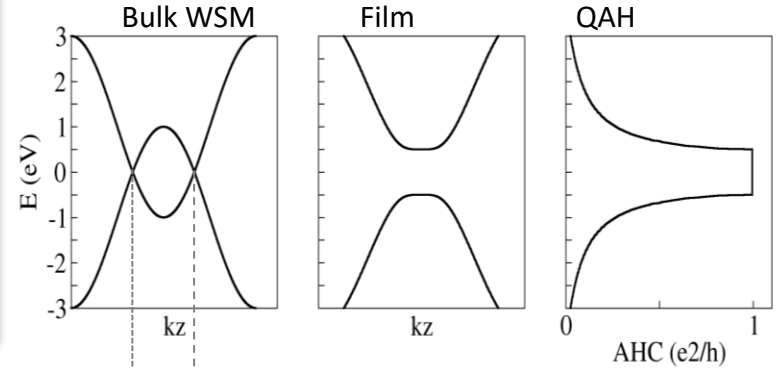
Co₂MnGa
Co₃Sn₂S₂
Mn₃Sn



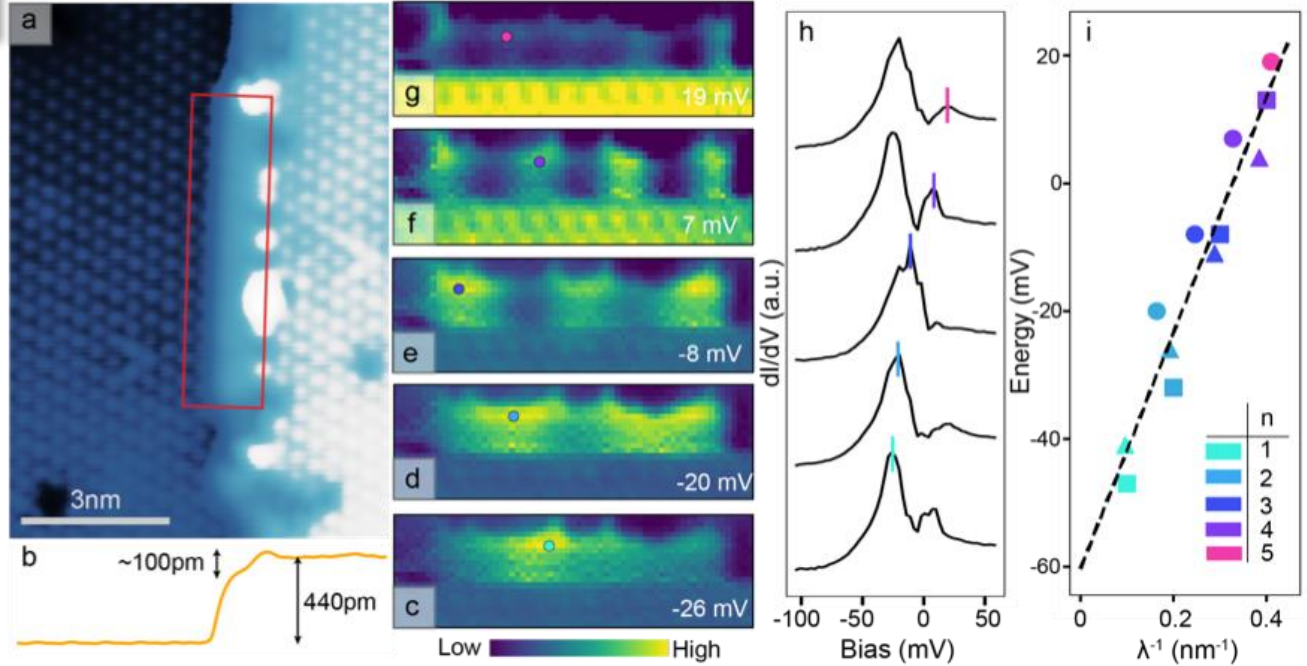
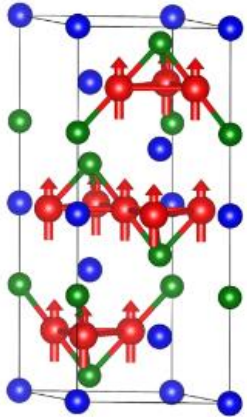
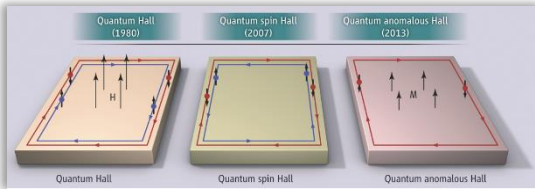
quantum devices



- Towards QAHE in MBE grown thin films.
- Magnetic Weyl for QAH effect in 2D



quantum anomalous Hall





new physics

- Berry phase design of materials for energy conversion and Hall sensors
- Quantum anomalous Hall effect at room temperature
- Berry curvature design in real and reciprocal space
- devices made of thin films and crystals

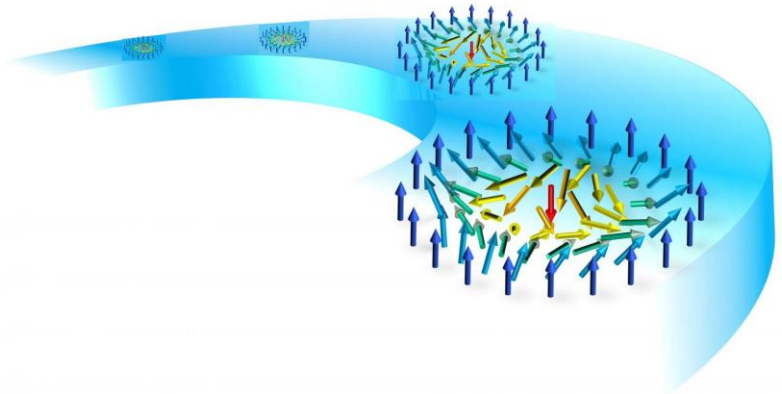
- potential applications

- spintronics

- Racetrack memory
- Majorana fermions
- Spin Hall based MRAM
- antiferromagnetic Spintronics
- Spin caloritronics

- quantum computing

- energy conversion



thank you for your attention



Yulin Chen
Stuart Parkin
and teams



Andrei
Bernevig
and Zahid
Hasan

